



Chen, J-H., Xu, W., & Sheppard, D. (2017). Altering intracellular pH reveals the kinetic basis of intraburst gating in the CFTR Cl⁻ channel. *Journal of Physiology*, 595(4), 1059–1076.
<https://doi.org/10.1113/JP273205>

Peer reviewed version

License (if available):
Unspecified

Link to published version (if available):
[10.1113/JP273205](https://doi.org/10.1113/JP273205)

[Link to publication record in Explore Bristol Research](#)
PDF-document

This is the author accepted manuscript (AAM). The final published version (version of record) is available online via Wiley at <http://onlinelibrary.wiley.com/doi/10.1113/JP273205/abstract>. Please refer to any applicable terms of use of the publisher.

University of Bristol - Explore Bristol Research

General rights

This document is made available in accordance with publisher policies. Please cite only the published version using the reference above. Full terms of use are available:
<http://www.bristol.ac.uk/red/research-policy/pure/user-guides/ebr-terms/>

**Altering intracellular pH reveals the kinetic basis of intraburst gating in the
CFTR Cl⁻ channel**

Jeng-Haur Chen^{1,2,3}, Weiyi Xu^{1,2} and David N. Sheppard³

¹School of Biomedical Sciences, ²HKU Shenzhen Institute of Research and Innovation,
University of Hong Kong, Hong Kong, China

and

³School of Physiology, Pharmacology and Neuroscience, University of Bristol, Bristol,
United Kingdom

Running title: *CFTR intraburst gating*

Address correspondence to Jeng-Haur Chen, School of Biomedical Sciences, HKU Shenzhen
Institute of Research and Innovation, University of Hong Kong, Li Ka Shing Faculty of
Medicine, Faculty of Medicine Building, 21 Sassoon Road, Pokfulam, Hong Kong, China.
Tel.: +852 3917 9512; Fax: +852 2855 9730; E-mail: jeng-haur-chen@hku.hk

Keywords: CFTR; chloride channel; cystic fibrosis

Words: 6648

Table of contents category: Molecular and cellular

KEY POINTS SUMMARY

- 1 • The cystic fibrosis transmembrane conductance regulator (CFTR), which is defective
2 in the genetic disease cystic fibrosis (CF), forms a gated pathway for chloride
3 movement regulated by intracellular ATP.
- 4 • To understand better CFTR function, we investigated the regulation of channel
5 openings by intracellular pH.
- 6 • We found that short-lived channel closures during channel openings represent subtle
7 changes in the structure of CFTR that are regulated by intracellular pH, in part, at
8 ATP-binding site 1 formed by the nucleotide-binding domains.
- 9 • Our results provide a framework for future studies to understand better the regulation
10 of channel openings, the dysfunction of CFTR in CF and the action of drugs that
11 repair CFTR gating defects.

ABSTRACT

Cystic fibrosis transmembrane conductance regulator (CFTR) is an ATP-gated Cl^- channel defective in the genetic disease cystic fibrosis (CF). The gating behaviour of CFTR is characterized by bursts of channel openings interrupted by brief, flickery closures, separated by long closures between bursts. Entry to and exit from an open burst is controlled by the interaction of ATP with two ATP-binding sites, sites 1 and 2 in CFTR. To understand better the kinetic basis of CFTR intraburst gating, we investigated the single-channel activity of human CFTR at different intracellular pH (pH_i) values. When compared with the control (pH_i 7.3), acidifying pH_i to 6.3 or alkalinizing pH_i to 8.3 and 8.8 caused small reductions in the open-time constant τ_o of wild-type CFTR. By contrast, the fast closed-time constant τ_{cf} , which describes the short-lived closures that interrupt open bursts, was greatly increased at pH_i 5.8 and 6.3. To analyse intraburst kinetics, we used linear three-state gating schemes. All data were satisfactorily modeled by the $C_1 \leftrightarrow O \leftrightarrow C_2$ kinetic scheme. Changing the intracellular ATP concentration was without effect on τ_o , τ_{cf} and their responses to pH_i changes. However, mutations that disrupt the interaction of ATP with ATP-binding site 1, including K464A, D572N and the CF-associated mutation G1349D all abolished the prolongation of τ_{cf} at pH_i 6.3. Taken together, our data suggest that the regulation of CFTR intraburst gating is distinct from the ATP-dependent mechanism that controls channel opening and closing. However, our data also suggest that ATP-binding site 1 modulates intraburst gating.

1 **ABBREVIATIONS**

2 ABC, ATP-binding cassette; CF, cystic fibrosis; CFTR, cystic fibrosis transmembrane
3 conductance regulator; IBI, interburst interval; MBD, mean burst duration; MSD, membrane-
4 spanning domain; NBD, nucleotide-binding domain; P_o , open probability; R domain,
5 regulatory domain.

1 INTRODUCTION

2 Cystic fibrosis transmembrane conductance regulator (CFTR) is an anion channel
 3 transporting Cl^- and HCO_3^- across the apical membrane of epithelial cells (Hwang & Kirk,
 4 2013). Structurally, CFTR belongs to the ATP-binding cassette (ABC) family, but
 5 distinctively it forms a ligand-gated ion channel (Hwang & Kirk, 2013). CFTR contains two
 6 membrane-spanning domains (MSDs) that form the channel pore, two nucleotide-binding
 7 domains (NBDs) that bind ATP molecules to control channel gating, and a unique regulatory
 8 domain (R domain) that confers CFTR activation by PKA-dependent phosphorylation
 9 (Hwang & Kirk, 2013). CFTR dysfunction causes the genetic disease cystic fibrosis (CF)
 10 (Riordan *et al.*, 1989). Because CF mutations frequently disrupt channel gating,
 11 understanding gating mechanisms in CFTR is important for deciphering the pathogenesis of
 12 CF and developing mutation-specific therapies.

13 The gating pattern of CFTR is characterized by bursts of openings interrupted by
 14 short-lived closures and separated by long closures between bursts (Anderson *et al.*, 1991;
 15 Winter *et al.*, 1994). Early studies demonstrated that the transition between long closures and
 16 bursts of openings is regulated by ATP binding and hydrolysis at the NBDs (Anderson *et al.*,
 17 1991; Hwang *et al.*, 1994; Carson *et al.*, 1995; Lansdell *et al.*, 1998; Zeltwanger *et al.*, 1999;
 18 Ikuma & Welsh, 2000; Vergani *et al.*, 2003). Later studies revealed that the two NBDs form
 19 a head-to-tail dimer with an interface containing two ATP-binding sites, site 1 and site 2
 20 (Lewis *et al.*, 2004; Vergani *et al.*, 2005). Evidence shows that the turnover rate of ATP at
 21 site 1 is less than that at site 2 in CFTR gating (Tsai *et al.*, 2009; Tsai *et al.*, 2010), because
 22 site 1 exhibits reduced or absent ATP hydrolytic activity (Aleksandrov *et al.*, 2002; Lewis *et*
 23 *al.*, 2004; Kidd *et al.*, 2004). With ATP stabilizing the two NBDs at site 1, NBD
 24 dimerization by ATP binding at site 2 powers CFTR opening (Vergani *et al.*, 2005).

Recent gating models suggest that site 2 cyclically binds and hydrolyzes ATP to drive channel gating (Aleksandrov *et al.*, 2002; Vergani *et al.*, 2005; Csanady *et al.*, 2010) at a slow pace, about once per second at room temperature (Li *et al.*, 1996). However, CFTR closing may not be strictly coupled to ATP hydrolysis as at least two open states are found to occur during channel opening (Hennager *et al.*, 2001; Jih *et al.*, 2012). In addition, significant structural rearrangement at site 1 may accompany the CFTR gating cycle induced by ATP binding and hydrolysis at site 2 (Csanady *et al.*, 2013), suggesting cross talk between sites 1 and 2 to regulate channel gating.

Most studies of CFTR gating have focused on transitions between the long closures and bursts of channel opening. The gating kinetics of short-lived channel closures within a burst have received less attention. Previous studies have attributed intraburst closures to recording noise, channel pore blockage by buffer ions such as HEPES (Dalemans *et al.*, 1991; Haws *et al.*, 1992; Tabcharani *et al.*, 1997; Zhou *et al.*, 2001) and MOPS (Ishihara & Welsh, 1997) or intrinsic conformational changes in CFTR itself (Ishihara & Welsh, 1997; Cai *et al.*, 2003). Intriguingly, the intraburst activity of CFTR resembles the gating behaviour of ligand-gated channels such as cyclic nucleotide-gated ion channels (Sunderman & Zagotta, 1999). Moreover, intraburst closures are sensitive to membrane voltage (Cai *et al.*, 2003) and temperature (Ishihara & Welsh, 1997) and differ between species (Lansdell *et al.*, 1998; Cai *et al.*, 2015). These data suggest that sequential openings and closings within a burst might be associated with kinetic shifts in CFTR conformation and modulated by physiological stimuli.

To test this hypothesis, we studied the single-channel kinetics of wild-type and mutant CFTR. Because intracellular pH (pH_i) alters CFTR gating (Chen *et al.*, 2009), we first tested whether intraburst activity is sensitive to different pH_i solutions. To investigate the underlying regulatory mechanisms for CFTR intraburst activity and its pH_i sensitivity, we

tested several well-known mutants, including the CF mutations $\Delta F508$, G551D and G1349D. Our data reveal that intraburst activity in CFTR is operated by an ATP-independent gating mechanism, but associated with the interaction of ATP at site 1. Our findings suggest that channel openings occur when CFTR enters the ATP-driven bursting state, wherein an ATP-independent mechanism closes the channel gate intermittently to generate short-lived intraburst closures.

METHODS

Cells and CFTR expression

Experimental details have been described previously (Chen *et al.*, 2009). Briefly, we used mammalian cells heterologously expressing human CFTR constructs. HeLa cells were used to transiently express K464A- and D572N-CFTR by the vaccinia virus/bacteriophage T7 hybrid expression system (Rich *et al.*, 1990) and wild-type and $\Delta F508$ -CFTR by plasmid transfection with Lipofectamine 2000 (Invitrogen) in some experiments. Other CFTR variants were stably expressed as follows: wild-type, $\Delta F508$ -, $\Delta RS660A$ - and G1349D-CFTR in mouse mammary epithelial (C127) cells; G551D-CFTR in Fischer rat thyroid (FRT) cells and K1250M-CFTR in NIH 3T3 cells. The single-channel behaviour of wild-type human CFTR in different mammalian cells is equivalent (Chen *et al.*, 2009).

Electrophysiology

CFTR currents in excised inside-out membrane patches were recorded using Axopatch 200A or 200B patch-clamp amplifiers and analyzed with pCLAMP software (all from Molecular Devices, Union City, CA, USA) as described previously (Sheppard & Robinson, 1997; Chen *et al.*, 2009). The pipette (extracellular) solution contained (mM): 140 N-methyl-D-glucamine (NMDG), 140 aspartic acid, 5 CaCl_2 , 2 MgSO_4 and 10 N-

[tris(hydroxymethyl)methyl]-2-aminoethanesulfonic acid (TES), pH 7.3 with Tris ($[\text{Cl}^-]$, 10 mM). The control bath (intracellular) solution contained (mM): 140 NMDG, 3 MgCl_2 , 1 CsEGTA , 5 Trizma base and 5 Bis-Tris, pH 7.3 with HCl, ($[\text{Cl}^-]$, 147 mM; free $[\text{Ca}^{2+}]$, $<10^{-8}$ M) at 37 °C. To ensure identical Cl^- concentrations, pH solutions were first titrated to pH 7.3 with HCl before titrating with H_2SO_4 to acidic pH or Tris to alkaline pH values.

CFTR channels in excised inside-out membrane patches were activated by adding PKA (75 nM) and ATP (1 mM) to the bath solution. Channel activity was maintained by adding fresh PKA (75 nM) and ATP (0.3 or 1 mM) at the start of each intervention. Membrane voltage was clamped at -50 mV. Experimental protocols and conditions were performed as described previously (Chen *et al.*, 2009). To augment the activity of CFTR mutants in the NBDs, we used ATP at 1 mM, whereas wild-type and ΔRS660A -CFTR were routinely studied using ATP at 0.3 mM. Most CFTR single-channel currents were initially recorded on digital audiotape (Biologic Scientific Instruments, model DTR-1204; Intracel Ltd., Royston, UK) at a bandwidth of 10 kHz, while some were directly digitized and stored in the computer. For digitization, recordings were filtered with an 8-pole Bessel filter (model 902LPF2 or 900; Frequency Devices, Inc., Ottawa, IL, USA) at a corner frequency (f_c) of 500 Hz and acquired using a Digidata 1200 or 1440 interface (Molecular Devices) and pCLAMP software at the sampling rate of 5 kHz. For the purpose of illustration, current recordings were filtered at 500 Hz and digitized at 1 kHz.

The number of active channels in a membrane patch was determined by the maximum number of recorded channels that opened simultaneously at any one time during the entire experiment. To obtain burst durations, the channel bursts formed by only one active channel were measured. For open probability (P_o) and burst analysis, event lists of open- and closed-times were created using pCLAMP software with a half-amplitude crossing criterion.

Transitions ≤ 1 ms were excluded from event lists (eight-pole Bessel filter rise time (T_{10-90}) ~ 0.73 ms at $f_c = 500$ Hz).

Single-channel open- and closed-time histograms were created using logarithmic x -axes with 10 bins per decade. Using the maximum likelihood method, open- and closed-time histograms were fitted with one- or two-component exponential functions, respectively. The mean values of exponential functions were used to derive open- and closed-time constants. P_o was calculated from open and closed times. To measure mean burst duration (MBD), interburst interval (IBI) and P_o within a burst ($P_{o\text{-burst}}$), burst analysis was performed using recordings from membrane patches that contained 1-4 active channels. The delimiter time (t_c) that separates interburst closures from intraburst closures was determined from the point of intersection between the two exponential curves fitting the fast and slow populations of channel closures in the closed-time histogram, as described previously (Carson *et al.*, 1995). Event lists and t_c values were used to derive MBD and $P_{o\text{-burst}}$ with pCLAMP software. Then, IBI was calculated using Equation 1:

$$P_o = \frac{\text{MBD} \times P_{o\text{-burst}}}{\text{MBD} + \text{IBI}} \quad \text{Equation (Eq.) 1}$$

To develop kinetic gating schemes, we used QuB software (www.qub.buffalo.edu; Qin *et al.*, 1997) with maximum likelihood analysis (Cai *et al.*, 2003), excluding transitions ≤ 1 ms. Only data from membrane patches that contained a single active channel were used for kinetic modeling.

Reagents and chemicals

With the exception of PKA purified from bovine heart (Promega, Southampton, UK and Calbiochem/Merck Millipore, Darmstadt, Germany), chemicals were purchased from the Sigma-Aldrich Company Ltd. (Gillingham, UK). Stock solutions of ATP were prepared fresh before each experiment.

Statistics

One-way ANOVA and paired Student's t-test were used to analyze sets of data. Differences were considered statistically significant when $P < 0.05$.

RESULTS

Acidic and alkaline intracellular solutions alter the intraburst activity of CFTR

To investigate the intraburst activity of the CFTR Cl^- channel, we studied the single-channel activity of wild-type human CFTR at different intracellular pH (pH_i) values from pH_i 5.8 to 8.8 (Fig. 1A and B). The gating pattern of CFTR is characterized by bursts of openings, separated by long closures and interrupted by short-lived closures within bursts (Fig. 1). Figures 1 and 2 and Table 1 demonstrate that pH_i had complex effects on CFTR channel gating. Consistent with our previous results (Chen *et al.*, 2009), the interburst activity of CFTR measured by open probability (P_o), mean burst duration (MBD) and interburst interval (IBI) had diverse responses to different pH_i solutions (Fig. 1 and Table 1). For example, at pH_i 6.3 P_o increased 1.5-fold because MBD increased 2.7-fold and IBI decreased 0.7-fold. By contrast, at pH_i 8.3 P_o decreased 0.7-fold because MBD decreased 0.6-fold and IBI increased 1.3-fold.

To examine whether intraburst openings and closings are sensitive to pH_i changes, we measured their dwell times using the open- and closed-time histograms (Fig. 2A-D). Our data demonstrate that the open-time constant (τ_o) was decreased ~0.8-fold at pH_i 6.3, pH_i 8.3 and pH_i 8.8, but unchanged at pH_i 5.8 (Fig. 2A, C and E). Of note, the fast closed-time constant (τ_{cf}), representing the population of short-lived intraburst closures in the closed-time histogram (Fig. 2B and D) was increased 1.6-fold at pH_i 6.3 and 1.5-fold at pH_i 5.8, but was

unaltered at alkaline pH_i (Fig. 2B, D and F). Thus, the data suggest that CFTR intraburst gating described by τ_o and τ_{cf} is sensitive to pH_i changes.

Consistent with the analysis of bursts (Table 1), pH_i had complex effects on the slow closed-time constant (τ_{cs}), representing the population of long interburst closures: τ_{cs} decreased 0.6-fold at pH_i 6.3, increased 3.7-fold at pH_i 5.8, increased 1.3-fold at pH_i 8.3, but was unaltered at pH_i 8.8 (Fig. 2B, D and G). Moreover, the diverse responses of τ_{cs} and τ_{cf} to different pH_i solutions suggest that the long interburst closures and short-lived intraburst closures might be regulated by distinct mechanisms.

Buffers are without effect on the intraburst activity of the CFTR Cl^- channel

A caveat for analyzing CFTR intraburst gating is that short-lived closures might result from blockage of the channel pore by buffer ions, such as HEPES (Dalemans *et al.*, 1991; Haws *et al.*, 1992; Tabcharani *et al.*, 1997; Zhou *et al.*, 2001), TES (Tabcharani *et al.*, 1997) and MOPS (Ishihara & Welsh, 1997). To address this possibility, we tested whether increasing the concentration of the buffers Trizma or Bis-Tris three-fold in the intracellular solution might alter CFTR intraburst gating (Fig. 3A-C). The data demonstrate that increasing the concentrations of either Trizma or Bis-Tris did not affect MBD, τ_o and τ_{cf} of wild-type CFTR (Fig. 3A-C). Similarly, using intracellular solutions with a different buffer, TES (10 mM), or the same Trizma buffer, but at a very low concentration (0.1 mM) had little or no effect on MBD, τ_o , τ_{cf} and τ_{cs} (Fig. 3D-G). Thus, the data suggest that intraburst closures were unlikely to be caused by buffer-generated blockage of the CFTR channel pore. Since the intraburst closures (Fig. 1) were also distinct from biphasic recording noise, the data suggest that openings and closings within a burst might represent stable and integral conformational states during CFTR gating.

1 Kinetic modeling of CFTR gating at different pH_i

2 Complex cyclic gating models have been developed to describe CFTR channel gating by
 3 ATP binding and hydrolysis at the NBDs (Tsai *et al.*, 2010; Jih *et al.*, 2012; Csanady *et al.*,
 4 2013). However, to investigate intraburst gating of CFTR at different pH_i, we utilized the
 5 simple linear three-state kinetic schemes $C_1 \leftrightarrow O \leftrightarrow C_2$ and $C_1 \leftrightarrow C_2 \leftrightarrow O$ to analyze
 6 transitions between the long closed state C_1 , short-lived closed state C_2 , and open state O (Fig.
 7 4A and F) (Winter *et al.*, 1994; Cai *et al.*, 2003). In both kinetic schemes, the rate constants
 8 β_1 , β_2 , α_1 and α_2 describe the transition rates between three gating states and bursts of channel
 9 opening are modeled by the transitions $O \leftrightarrow C_2$ or $C_2 \leftrightarrow O$ (Fig. 4A and F, see dashed boxes).
 10 In the $C_1 \leftrightarrow O \leftrightarrow C_2$ kinetic scheme, the relationships between the rate constants and other
 11 kinetic parameters can be described by Equation 2 (Colquhoun & Hawkes, 1982; Sakmann &
 12 Trube, 1984):

$$13 \quad \text{IBI} = \tau_{cs} = \frac{1}{\beta_1}; \text{MBD} = \frac{(\beta_2 + \alpha_2)}{\alpha_1 \alpha_2}; \tau_{cf} = \frac{1}{\alpha_2}; \tau_o = \frac{1}{\alpha_1 + \beta_2} \quad \text{Eq. 2}$$

14 In the $C_1 \leftrightarrow O \leftrightarrow C_2$ kinetic scheme, an increase in the rate constant β_1 at pH_i 6.3 (Fig.
 15 4B) decreased IBI (Table 1) and τ_{cs} (Fig. 2G), whereas reductions in β_1 at pH_i 8.3 and 5.8
 16 (Fig. 4B) enhanced IBI and τ_{cs} at these pH_i values (Table 1 and Fig. 2G). In addition,
 17 decreases in α_1 prolonged MBD at acidic pH_i 5.8 and 6.3 (Fig. 4D and Table 1), whereas
 18 increases in α_1 shortened MBD at alkaline pH_i 8.3 and 8.8 (Fig. 4D and Table 1). For CFTR
 19 intraburst gating, the increased β_2 rate constant at pH_i 6.3 (Fig. 4C) might cause a small
 20 decrease in τ_o (Fig. 2E) as $\tau_o = 1/(\alpha_1 + \beta_2)$ (Eq. 2). Following this equation, the enhanced α_1
 21 rate constant at alkaline pH_i (Fig. 4D) might also cause a small reduction in τ_o (Fig. 2E).
 22 Moreover, the marked increase in τ_{cf} at acidic pH_i 6.3 and 5.8 (Fig. 2F) might be caused by
 23 large reductions in the α_2 rate constant (Fig. 4E) as $\tau_{cf} = 1/\alpha_2$ (Eq. 2). Taken together, these
 24 data suggest that the $C_1 \leftrightarrow O \leftrightarrow C_2$ kinetic scheme adequately accounts for the pH_i-
 25 sensitivity of CFTR interburst and intraburst gating.

Because the $C_1 \leftrightarrow O \leftrightarrow C_2$ and $C_1 \leftrightarrow C_2 \leftrightarrow O$ kinetic schemes are mathematically equivalent (Colquhoun & Hawkes, 1982; Sakmann & Trube, 1984; Kienker, 1989), we next modeled CFTR gating using the $C_1 \leftrightarrow C_2 \leftrightarrow O$ kinetic scheme. In the $C_1 \leftrightarrow C_2 \leftrightarrow O$ kinetic scheme, the relationships between rate constants and kinetic parameters can be described by Equation 3 (Colquhoun & Hawkes, 1982; Sakmann & Trube, 1984):

$$IBI = \tau_{cs} = \frac{1}{\beta_1} \left[1 + \left(\frac{\alpha_1}{\beta_2} \right) \right] + \left(\frac{1}{\beta_2} \right); \text{MBD} = \frac{(\beta_2 + \alpha_1)^2 + \beta_2 \alpha_2}{(\beta_2 + \alpha_1) \alpha_1 \alpha_2}; \tau_{cf} = \frac{1}{\alpha_1 + \beta_2}; \tau_o = \frac{1}{\alpha_2} \quad \text{Eq. 3}$$

Consistent with the $C_1 \leftrightarrow O \leftrightarrow C_2$ kinetic scheme (Fig. 4B and D), alterations in β_1 and α_1 in the $C_1 \leftrightarrow C_2 \leftrightarrow O$ kinetic scheme (Fig. 4G and I) accounted for the changes in IBI and MBD, respectively, at different pH_i (Eq. 3 and Table 1). However, the rate constants β_2 and α_2 , which describe intraburst gating in this scheme were little altered at different pH_i (Fig. 4H and J). Instead, the $C_1 \leftrightarrow C_2 \leftrightarrow O$ kinetic scheme indicated that alterations in τ_{cf} at different pH_i (Fig. 2F) were caused by the corresponding changes in the rate constant α_1 (Fig. 4I) as $\tau_{cf} = 1/(\alpha_1 + \beta_2)$ (Eq. 3). Moreover, the small decreases in τ_o at pH_i 6.3, 8.3 and 8.8 (Fig. 2E) were not well simulated by the rate constant α_2 in the $C_1 \leftrightarrow C_2 \leftrightarrow O$ kinetic scheme (Fig. 4J).

To further compare the modeling results of these two kinetic schemes (Fig. 4) with the measured data in Figure 2 and Table 1, we derived the kinetic parameters P_o , P_o within a burst ($P_{o\text{-burst}}$), MBD, IBI, τ_o , τ_{cf} and τ_{cs} (Tables 2 and 3) using the rate constant data at acidic pH_i 6.3 and 5.8 (Fig. 4). At pH_i 6.3 and 5.8, we observed large changes in CFTR intraburst gating (Fig. 1 and 2). Tables 2 and 3 demonstrate that the kinetic parameters derived using both schemes at pH_i 6.3 and 5.8 were comparable to our measured data. However, the τ_o value derived by the $C_1 \leftrightarrow C_2 \leftrightarrow O$ kinetic scheme was not significantly decreased at pH_i 6.3 compared to that at pH_i 7.3 (Table 3), consistent with the modeling results (Fig. 4J). To interpret these data, we speculate that although mathematically the two kinetic schemes generate similar modeling results, the kinetic relationship between the three gating states

might prevent the $C_1 \leftrightarrow C_2 \leftrightarrow O$ kinetic scheme from adequately modeling pH_i -sensitive changes in CFTR intraburst gating.

As the $C_1 \leftrightarrow O \leftrightarrow C_2$ kinetic scheme consistently well described pH_i -sensitive intraburst gating of CFTR, we selected this kinetic scheme to analyse data acquired in subsequent experiments. Because CFTR gating is ATP-dependent (Hwang & Kirk, 2013), we began by testing whether the pH_i -sensitive intraburst activity of CFTR is regulated by the ATP concentration. For these experiments, we studied channel gating at pH_i 6.3, because it induced significant changes in CFTR intraburst activity (Figs. 1 and 2).

ATP-dependence of acid-sensitive intraburst gating

Numerous studies have demonstrated that the opening rate of CFTR or the rate constant β_1 in the $C_1 \leftrightarrow O \leftrightarrow C_2$ kinetic scheme is ATP-dependent (Winter *et al.*, 1994; Venglarik *et al.*, 1994; Li *et al.*, 1996; Zeltwanger *et al.*, 1999; Cai & Sheppard, 2002; Vergani *et al.*, 2003). Previous studies (Winter *et al.*, 1994; Li *et al.*, 1996; Lansdell *et al.*, 1998) also demonstrate that τ_o and τ_{cf} are independent of the intracellular ATP concentration. Nevertheless, some data raise the possibility that intraburst gating might be ATP-dependent (Zeltwanger *et al.*, 1999; Cai & Sheppard, 2002; Cai *et al.*, 2015).

Figure 5 demonstrates the effects of different ATP concentrations on CFTR gating at pH_i 6.3 and 7.3. At both pH_i 7.3 and 6.3, τ_{cs} was markedly decreased from 0.03 to 0.3 mM ATP and further reduced from 0.3 to 1 mM ATP (Fig. 5B). Interestingly, τ_{cs} at pH_i 6.3 was smaller than that at pH_i 7.3 in the presence of ATP at 0.3 and 1 mM, but not at 0.03 mM, (Fig. 5B), suggesting that when the ATP concentration is very low, the collision frequency of ATP molecules with CFTR becomes the rate-limiting factor for channel opening. When compared to values at pH_i 7.3, the effects of pH_i 6.3 on τ_o and τ_{cf} were similar among all three ATP concentrations tested (Fig. 5D-E). Interestingly, values of MBD were significantly prolonged

at pH_i 6.3 compared to those at pH_i 7.3, particularly at 0.3 and 1 mM ATP (Fig. 5C), suggesting that the ATP collision rate might affect the stability of CFTR's bursting state at acidic pH_i . Consistent with the τ_{cs} changes (Fig. 5B), only the rate constant β_1 in the $C_1 \leftrightarrow O \leftrightarrow C_2$ kinetic scheme was sensitive to the ATP concentration (Fig. 5F-I).

Conversely, the kinetic parameters for CFTR intraburst gating including the time constants τ_o and τ_{cf} (Fig. 5D and E) and rate constants β_2 and α_2 (Fig. 5H and I) were insensitive to the ATP concentration at both pH_i 7.3 and 6.3, suggesting that intraburst openings and closings are not regulated by ATP. However, it is uncertain whether the intraburst closings might represent the intermediate closed state when CFTR has already bound ATP prior to channel opening (Haws *et al.*, 1992; Venglarik *et al.*, 1994; Zeltwanger *et al.*, 1999). Using the two linear kinetic schemes (Fig. 4A and F), we examined this possibility by analyzing chemical kinetics (see Appendix A) to mathematically derive the relationship between the P_o of CFTR and the ATP concentration, which is best described by the Michaelis-Menten equation (Anderson *et al.*, 1991; Venglarik *et al.*, 1994; Zeltwanger *et al.*, 1999; Cai & Sheppard, 2002; Vergani *et al.*, 2003; Scott-Ward *et al.*, 2007; Chen *et al.*, 2009). The modeling results show that both kinetic models required an intermediate closed state C_1' between the long closed state C_1 and the bursting state to derive a Michaelis-Menten-like relationship (e.g. the $C_1 \leftrightarrow C_1' \leftrightarrow O \leftrightarrow C_2$ kinetic scheme in Appendix A, Eq. A7 for the $C_1 \leftrightarrow O \leftrightarrow C_2$ kinetic scheme). Therefore, the short-lived C_2 state is unlikely to represent an ATP-bound intermediate closed state in CFTR gating. These data also suggest that CFTR intraburst gating might be controlled by a gating mechanism that follows ATP binding to CFTR.

Next, we explored whether the interaction of ATP molecules with ATP-binding sites 1 and 2 affects the intraburst activity of CFTR. For these experiments, we studied several CFTR mutants in the NBDs that disturb ATP binding and hydrolysis.

Role of the R domain and ATP-binding sites in CFTR intraburst gating

To disrupt ATP-dependent regulation of CFTR channel gating, we selected four CFTR variants (Fig. 6 and 7): (i) Δ RS660A-CFTR, which deletes a large part of the R domain and likely impacts the function of both ATP-binding sites (Rich *et al.*, 1991; Winter & Welsh, 1997; Mense *et al.*, 2006); (ii) K1250M-CFTR, which impairs ATP binding and hydrolysis at site 2 (Carson *et al.*, 1995; Vergani *et al.*, 2003; Vergani *et al.*, 2005); (iii) K464A-CFTR, which perturbs ATP binding at site 1 (Carson *et al.*, 1995; Vergani *et al.*, 2003) and (iv) D572N-CFTR, which attenuates Mg^{2+} binding at site 1 (Vergani *et al.*, 2003).

Figure 6 shows representative recordings (Fig. 6A), τ_o and τ_{cf} data (Fig. 6B and C) of Δ RS660A-CFTR tested at pH_i 7.3 and pH_i 6.3 in the presence of 0.3 mM ATP. Compared to that of wild-type CFTR, τ_o was reduced, but τ_{cf} was enhanced in Δ RS660A-CFTR at pH_i 7.3 (see # symbols, Fig. 6B and C). However, similar to that in wild-type CFTR, pH_i 6.3 decreased τ_o but increased τ_{cf} of Δ RS660A-CFTR (Fig. 6B and C). Moreover, Figure 7 shows representative recordings, τ_o and τ_{cf} data of CFTR NBD mutants at pH_i 7.3 and pH_i 6.3 in the presence of 1 mM ATP. When compared with values for wild-type CFTR, the τ_o of K464A-CFTR at pH_i 7.3 was decreased (Fig. 7B), whereas the K1250M mutation appeared to decrease τ_o ($P = 0.12$), but increase τ_{cf} ($P = 0.08$) at pH_i 7.3 (Fig. 7B and C). Interestingly, the τ_o reduction by pH_i 6.3 in wild-type CFTR was abolished by the NBD mutations K1250M, K464A and D572N (Fig. 7B), whereas the τ_{cf} elongation by pH_i 6.3 was absent in the mutants K464A- and D572N-CFTR (Fig. 7C). We interpret these results to suggest that the R domain and ATP-binding sites might contribute to the regulation of CFTR intraburst gating. The data also suggest that both ATP-binding sites might contribute to the reduction in τ_o at pH_i 6.3, whereas only site 1 might mediate the prolongation of τ_{cf} at pH_i 6.3.

1 The CF mutation G1349D greatly disturbs CFTR intraburst gating

2 To further investigate the roles of ATP-binding sites 1 and 2 and learn whether CF mutations
 3 perturb intraburst gating, we studied the CF mutations, Δ F508, G551D and G1349D at 1 mM
 4 ATP (Fig. 8). Located on the surface of NBD1, Δ F508 not only perturbs communication
 5 between the NBDs and MSDs (Serohijos *et al.*, 2008; Mornon *et al.*, 2008; Dong *et al.*, 2011),
 6 but also destabilizes the NBD1:NBD2 dimer (Jih *et al.*, 2011). By contrast, G551D and
 7 G1349D affect equivalent residues in the LSGGQ motifs in NBD1 and NBD2, which
 8 contribute to site 2 and site 1, respectively (Lewis *et al.*, 2004; Cai *et al.*, 2006; Bompadre *et al.*, 2007). Both mutations perturb severely CFTR channel gating, with G551D rendering
 9 CFTR gating ATP-independent (Bompadre *et al.*, 2007).

11 Consistent with previous studies (Cai *et al.*, 2006), G551D and G1349D not only
 12 greatly prolonged IBI, but noticeably reduced the MBD of CFTR (Fig. 8A and B).
 13 Interestingly, pH_i 6.3 only enhanced the MBD of Δ F508-CFTR among the three CF mutants
 14 studied (Fig. 8B). However, the fold change of MBD in Δ F508-CFTR was less than that of
 15 wild-type CFTR (MBD_{pH_i 6.3}/MBD_{pH_i 7.3}: Δ F508-CFTR, 1.8 ± 0.2 ; wild-type CFTR, 2.8 ± 0.2 ;
 16 $N = 6$, $P < 0.05$, one-way ANOVA; Fig. 8B). Of note, at pH_i 6.3 the MBD of G1349D-
 17 CFTR was significantly reduced (Fig. 8A and B).

18 For CFTR intraburst gating, only G1349D caused large reductions in both τ_o and τ_{cf} at
 19 pH_i 7.3 (Fig. 8C and D). Like wild-type CFTR, the τ_o of all three CF mutants at pH_i 6.3 was
 20 shorter than that at pH_i 7.3 (Fig. 8C, $P = 0.061$ for G551D). However, only G551D and
 21 G1349D abolished the prolongation of τ_{cf} at pH_i 6.3 (Fig. 8D). Moreover, the MBD/ τ_o ratio,
 22 which is used to estimate the average number of channel openings within a burst of openings
 23 was unchanged in Δ F508-CFTR compared to that of wild-type CFTR (Fig. 8E). Conversely,
 24 the MBD/ τ_o ratio at both pH_i 7.3 and pH_i 6.3 was reduced to 1.7 in G551D-CFTR and 1.3 in
 25 G1349D-CFTR compared to 2.8 at pH_i 7.3 for wild-type CFTR (see # symbols, Fig. 8E).

These data suggest that bursts of channel openings were very difficult to form in G1349D-CFTR such that each burst often only appeared to contain a single opening (Fig. 8A). Taken together, our data indicate that CFTR intraburst gating and its pH_i -sensitivity were altered slightly by ΔF508 , moderately by G551D, but severely by G1349D.

DISCUSSION

This study aimed to investigate intraburst gating in the CFTR Cl^- channel by exploiting the effects of pH_i on gating kinetics. Our data reveal that intraburst openings and closings are integral gating events. The $\text{C}_1 \leftrightarrow \text{O} \leftrightarrow \text{C}_2$ kinetic scheme adequately simulated CFTR intraburst gating at different pH_i values. Mutations in ATP-binding site 1, particularly the CF mutation G1349D, had greater impact on intraburst gating than those in ATP-binding site 2.

Nature of the intraburst closures

When recording the single-channel activity of CFTR, we and other groups (e.g. Ishihara & Welsh, 1997; Tabcharani *et al.*, 1997; Vergani *et al.*, 2005; Fuller *et al.*, 2005; Bompadre *et al.*, 2007) consistently observed burst-like openings when the channel is open. Most studies attribute this bursting behaviour of CFTR to the brief and intermittent intraburst closures, which interrupt channel openings. It is proposed that these intraburst closures are caused by blockage of the CFTR pore by buffer ions (Ishihara & Welsh, 1997; Tabcharani *et al.*, 1997; Zhou *et al.*, 2001) or unknown intrinsic conformational movements (Ishihara & Welsh, 1997; Cai *et al.*, 2003). Studies using open-channel blockers of CFTR have demonstrated that fast-speed channel blockers with low binding affinity (e.g. niflumic acid, Scott-Ward *et al.*, 2004) only intermittently and partially obstruct Cl^- flow through the channel pore. Conversely, intermediate-speed channel blockers with high binding affinity (e.g. glibenclamide, Sheppard & Robinson, 1997) cause full blockage of CFTR single-channel currents. The buffer ion best

known to block the CFTR pore is MOPS, which shows fast and intermediate-speed blocking behaviour at 10 mM (Ishihara & Welsh, 1997). These studies together with the present data argue that the millimolar concentrations of buffer ions in our intracellular solutions are unlikely to cause open-channel block of the CFTR pore when the channel is open. Recording noise, often seen as biphasic spikes, are unlikely to be the reason for intraburst closures. Interestingly, the short-lived closures are sensitive to the membrane voltage (Zhou *et al.*, 2001; Cai *et al.*, 2003). Therefore, we speculate that part of the conformational changes that underlie CFTR intraburst gating occur within the MSDs.

Control of the intraburst activity in CFTR gating

NBD dimerization and dissociation induced by cycles of ATP binding and hydrolysis at binding site 2 forms the basic gating mechanism for interburst gating of the CFTR Cl^- channel (Vergani *et al.*, 2005; Scott-Ward *et al.*, 2007; Tsai *et al.*, 2010; Csanady *et al.*, 2010; Jih *et al.*, 2012). Interestingly, our study found that the effects of pH_i , ATP and mutations on intraburst gating (τ_o and τ_{cf}) of CFTR were mismatched to their effects on interburst gating such as τ_{cs} , IBI and MBD. These findings suggest the presence of a second gating mechanism that controls CFTR intraburst gating. We propose that once CFTR enters the open state during ATP-dependent gating cycles, the second gating mechanism intermittently closes the channel pore thereby generating fast and short-lived intraburst closures.

Several lines of evidence support the presence of a second gating mechanism governing the intraburst activity of CFTR. First, previous work demonstrates that disrupting salt bridges in the MSDs alters the intraburst activity of CFTR (Cotten & Welsh, 1999). Mutations on extracellular loop 1 in MSDs could destabilize the burst duration of CFTR (Sheppard *et al.*, 1993; Cui *et al.*, 2014; Infield *et al.*, 2016). Second, studies of CFTR homologues have identified differences in intraburst gating (Lansdell *et al.*, 1998; Scott-Ward

et al., 2007). Differences in the MSDs are likely responsible for the peculiar patterns of intraburst gating between murine and human CFTR (Scott-Ward *et al.*, 2007). Similarly, ovine CFTR exhibits differences in intraburst gating to human CFTR characterized by shorter τ_{cf} , but longer τ_o than human CFTR (Cai *et al.*, 2015). Finally, while studying the permeation of $[\text{Au}(\text{CN})_2]^{-1}$ through the channel pore of cysless-CFTR, a gate movement within a defined section of the MSDs encompassing residues 338-341 in transmembrane segment 6 was discovered recently (Gao & Hwang, 2015). These data suggest that the gating mechanism which controls the intraburst activity of CFTR varies among different species and is possibly associated with conformational changes in the MSDs.

pH_i sensitivity of CFTR intraburst gating

Interburst closures demonstrate a different sensitivity to pH_i changes than intraburst closures. Our previous work suggest that ATP-binding site 2 determines the pH_i sensitivity of MBD and IBI in CFTR gating (Chen *et al.*, 2009). Because G1349D-CFTR may have modest ATP function at site 2 (Cai *et al.*, 2006; Bompadre *et al.*, 2007), large alterations in its intraburst activity and pH_i sensitivity are plausibly caused by ATP dysfunction at binding site 1. The site 1 mutations K464A and D572N, which prevented the τ_{cf} prolongation at pH_i 6.3 may also have normal ATP function at site 2 (Vergani *et al.*, 2003). Therefore, our data suggest that ATP-binding site 1 plays a major role in sensing acidic pH_i during CFTR intraburst gating.

Several studies demonstrate that ATP binding at site 1 regulates CFTR gating by acting like a ligand. At site 1, ATP has a higher binding affinity than site 2 (Howell *et al.*, 2000), but exhibits a low turnover rate (i.e. over ten minutes) in biochemical studies (Aleksandrov *et al.*, 2002; Basso *et al.*, 2003) and shows reduced or no hydrolytic activity (Aleksandrov *et al.*, 2002; Lewis *et al.*, 2004; Kidd *et al.*, 2004). Conversely, patch-clamp studies indicate that ATP turnover at site 1 might be less than a minute or a few seconds (Tsai

et al., 2009; Tsai *et al.*, 2010), suggesting that ATP stability at binding site 1 during active CFTR gating cycles might be less than that in the biochemical studies (Aleksandrov *et al.*, 2002; Basso *et al.*, 2003). Consistent with this idea, Csanady *et al.* (2013) found that site 1 undergoes significant structural rearrangements during channel opening. Thus, CFTR intraburst gating might resemble that of the cyclic nucleotide-gated channels (Sunderman & Zagotta, 1999), in which unstable binding of the ligand causes dynamic conformational rearrangements that generate the intermittent intraburst closures. Moreover, amino acid residues such as H620, H667, C469 and C491 around the K464 and D572N residues at ATP-binding site 1 might be candidates for sensing pH_i changes. Future studies should explore their potential role in CFTR intraburst gating.

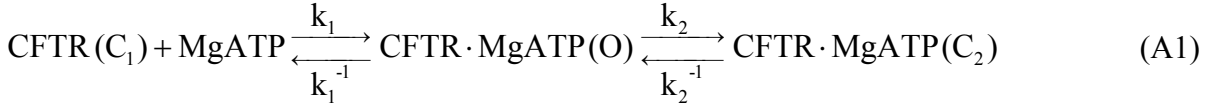
By contrast, whether CFTR intraburst gating requires normal ATP function at site 2 is uncertain. This query is raised because the G551D mutation greatly impairs the ATP-dependence of channel gating at site 2 (Cai *et al.*, 2006; Bompadre *et al.*, 2007), but it only showed mild effects on CFTR intraburst gating. Intriguingly, G551D-CFTR still responds to gating potentiators, such as genistein and phloxadine B (Illek *et al.*, 1999; Cai *et al.*, 2006), which enhance CFTR activity possibly by restoring NBD dimerization around site 2 (Cai *et al.*, 2006; Zegar-Moran *et al.*, 2007). Therefore, we speculate that in our recording condition, sporadic ATP binding or NBD dimerization by an unknown ATP-independent mechanism at site 2 might eventually transform G551D-CFTR into the bursting state, which is required for initiating intraburst gating by a second gating mechanism. Similarly, mutations that greatly prolong the channel opening rate such as K1250M (Carson *et al.*, 1995), G551D (Cai *et al.*, 2006) and ΔF508 (Dalemans *et al.*, 1991) only mildly or slightly affected CFTR intraburst gating.

In conclusion, our study characterized the kinetic basis of intraburst gating in CFTR by changing different pH_i solutions. The data suggest that a separate gating mechanism

operating together with the ATP-driven NBD dimerization model (Vergani *et al.*, 2005; Hwang & Kirk, 2013) is required for CFTR intraburst gating. While highlighting the complexity of CFTR gating, this study leaves some unresolved aspects of intraburst gating to future studies. For example, the mechanism that generates two short-lived closed states in CFTR intraburst gating at room temperature (Ishihara & Welsh, 1997) remains unclear. Nevertheless, this work emphasizes the importance of analysing intraburst activity to understand fully the CFTR gating mechanism. We suggest that ATP-dependent channel activity in CFTR represents cycles of transitions between the long closed state and bursting state, whereas movement of a channel gate during the bursting state might be investigated by studying intraburst gating.

APPENDIX A: ATP-dependence of the $C_1 \leftrightarrow O \leftrightarrow C_2$ kinetic scheme

Equation A1 (Eq. A1) describes ATP-dependent CFTR gating using the $C_1 \leftrightarrow O \leftrightarrow C_2$ kinetic scheme:



where k_1 , k_1^{-1} , k_2 and k_2^{-1} are the rate constants and $CFTR \cdot MgATP$ represents CFTR with bound MgATP. The rate constant k_1 describes the ATP-dependent opening rate of CFTR, whereas the rate constant k_1^{-1} indicates the closing rate of CFTR due to ATP hydrolysis or release. The rate constants k_2 and k_2^{-1} are used to describe the static transitions of CFTR intraburst gating. Following Eq. A1, we can obtain P_o from Eq. A2:

$$P_o = \frac{T_o}{T_{C_1} + T_{C_2} + T_o} \quad (A2)$$

where the dwell times T_{C_1} , T_{C_2} and T_o represent the time CFTR spends in the three kinetic states C_1 , C_2 and O , respectively. Assuming that the three kinetic states remain in equilibrium, the forward and reverse reaction rates between the two connected states are the same (Eq. A3):

$$k_1 \times (T_{C_1} \cdot [MgATP]) = k_1^{-1} \times T_o; \quad k_2 \times T_o = k_2^{-1} \times T_{C_2} \quad (A3)$$

Therefore, P_o is derived using Eq. A2 and A3:

$$P_o = \frac{1}{1 + \frac{k_1^{-1}}{k_1 \cdot [MgATP]} + \frac{k_2}{k_2^{-1}}} = \frac{\frac{k_2^{-1}}{k_2 + k_2^{-1}} [MgATP]}{[MgATP] + \frac{k_1^{-1} \cdot k_2^{-1}}{k_1(k_2 + k_2^{-1})}} \quad (A4)$$

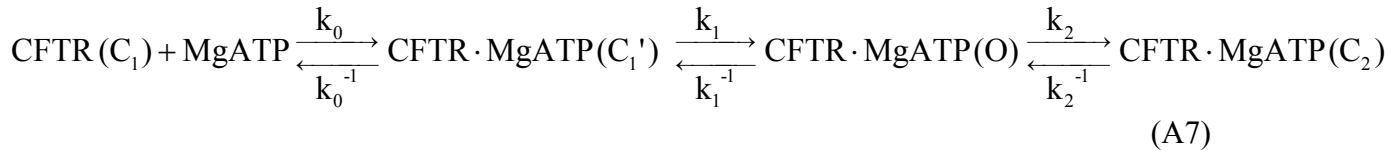
$$\text{Consequently, as } [MgATP] \rightarrow \infty, \text{ the maximum } P_o (P_{o\max}) = \frac{k_2^{-1}}{k_2 + k_2^{-1}}$$

Although Eq. A4 describes the hyperbolic relationship between [MgATP] and the P_o of CFTR similar to the Michaelis-Menten equation (see below Eq. A6 with a constant K), $P_{o\max}$ will be close to the P_o within a burst ($P_{o\text{-burst}}$, Table 2) ~ 0.9 , which is higher than our previous data ~ 0.72 at pH_i 7.3 (Chen *et al.*, 2009). A similar result was also found for the $C_1 \leftrightarrow C_2 \leftrightarrow O$ kinetic scheme (data not shown).

$$P_o = \frac{P_{o\max}[\text{MgATP}]}{[\text{MgATP}] + K} \quad (\text{Michaelis-Menten equation}) \quad (\text{A6})$$

A possible reason for this discrepancy is that after ATP binding to CFTR, there might be an intermediate, rate limiting state prior to the ATP-dependent conformational changes that lead to channel opening (Haws *et al.*, 1992; Venglarik *et al.*, 1994), i.e. the conformational changes for NBD dimerization (Vergani *et al.*, 2005) and coupling of the NBDs and MSDs (Hwang & Kirk, 2013).

To model this ATP-dependent rate-limiting step, we added an additional gating state C_1' with the rate constants k_0 and k_0^{-1} between the C_1 and O states (the $C_1 \leftrightarrow C_1' \leftrightarrow O \leftrightarrow C_2$ kinetic scheme, Eq. A7).



The P_o and $P_{o\max}$ for Eq. A7 can be derived from the following equations (Eqs. A8-A11) with $T_{C_1'}$ representing the dwell time CFTR spends in the C_1' state:

$$P_o = \frac{T_o}{T_{C_1} + T_{C_1'} + T_{C_2} + T_o} \quad (\text{A8})$$

$$k_0 \times (T_{C_1} \cdot [\text{MgATP}]) = k_0^{-1} \times T_{C_1'}; \quad k_1 \times T_{C_1'} = k_1^{-1} \times T_o; \quad k_2 \times T_o = k_2^{-1} \times T_{C_2} \quad (\text{A9})$$

$$P_o = \frac{\frac{1}{(1 + \frac{k_1^{-1}}{k_1} + \frac{k_2^{-1}}{k_2})} [\text{MgATP}]}{[\text{MgATP}] + \frac{k_0^{-1} \cdot k_1^{-1} \cdot k_2^{-1}}{k_0 \cdot (k_1 \cdot k_2^{-1} + k_1^{-1} \cdot k_2^{-1} + k_2 \cdot k_1)}} \quad (\text{A10})$$

$$P_{\text{omax}} = \frac{1}{(1 + \frac{k_1^{-1}}{k_1} + \frac{k_2^{-1}}{k_2})} \quad (\text{A11})$$

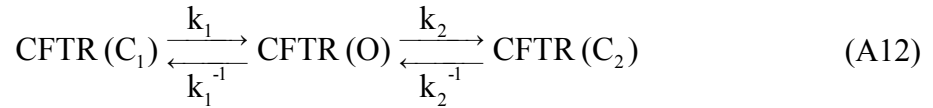
Our calculations show that the relationship between P_o and $[\text{MgATP}]$ is well described by the Michaelis-Menten-like equation (Eq. A10) with P_{omax} (Eq. A11) containing the k_1 rate constant as the rate-limiting parameter. Moreover, Eq. A11 suggests that the P_{omax} of CFTR might be close to $P_{o\text{-burst}}$ only if the rate constant k_1^{-1} is close to zero causing a permanent bursting state, or if the rate constant k_1 becomes infinite eliminating the rate-limiting step ($C_1' \rightarrow O$). By a similar approach, we also derived the $C_1 \leftrightarrow C_1' \leftrightarrow C_2 \leftrightarrow O$ kinetic scheme from the $C_1 \leftrightarrow C_2 \leftrightarrow O$ kinetic scheme (data not shown).

Previous work (Venglarik *et al.*, 1994) applying noise analysis to macroscopic current recordings of wild-type CFTR demonstrated that the $C_1 \leftrightarrow C_1' \leftrightarrow O$ kinetic scheme, excluding short-lived closures, well models the ATP-dependent channel activity of CFTR using the Michaelis-Menten relationship. Their modeling results (Venglarik *et al.*, 1994) also suggest that when the $C_1' \leftrightarrow O$ transitions are rate limiting, a single population of the long closures (Fig. 2B and D) was achieved in the $C_1 \leftrightarrow C_1' \leftrightarrow O$ kinetic scheme. Interestingly, recent studies identified the presence of transient closed states in the journey from long closures to channel openings (Scott-Ward *et al.*, 2007; Sorum *et al.*, 2015). These transient closed states, if rate limiting, are consistent with the C_1' state supporting CFTR gating with the Michaelis-Menten relationship.

Many studies have developed complex loop models with multiple substates within the $C_1 \leftrightarrow O$ transition controlled by ATP binding and hydrolysis (Vergani *et al.*, 2005; Scott-

Ward *et al.*, 2007; Tsai *et al.*, 2009; Tsai *et al.*, 2010; Csanady *et al.*, 2010; Jih *et al.*, 2012; Sorum *et al.*, 2015). The transition rates between the C₁ and O states in the C₁ ↔ O ↔ C₂ kinetic scheme should represent the overall transition rates through these multiple substates. Thus, we did not further investigate more complex gating schemes in this study.

Finally, to verify our approach, we calculated P_o from the C₁ ↔ O ↔ C₂ kinetic scheme without MgATP (Eqs. A12-14).



$$k_1 \times T_{C_1} = k_1^{-1} \times T_O; \quad k_2 \times T_O = k_2^{-1} \times T_{C_2} \quad (\text{A13})$$

$$P_o = \frac{T_O}{T_O + T_{C_1} + T_{C_2}} = \frac{1}{1 + \left(\frac{k_1^{-1}}{k_1}\right) + \left(\frac{k_2^{-1}}{k_2}\right)} = \frac{k_1 \cdot k_2^{-1}}{(k_1 + k_1^{-1})(k_2 + k_2^{-1}) - k_2 \cdot k_1^{-1}} \quad (\text{A14})$$

Our calculations derive P_o (Eq. A14) in a similar way to that reported previously (Sakmann & Trube, 1984), validating our mathematical approach using chemical kinetics.

REFERENCES

- Aleksandrov L, Aleksandrov AA, Chang XB, & Riordan JR (2002). The first nucleotide binding domain of cystic fibrosis transmembrane conductance regulator is a site of stable nucleotide interaction, whereas the second is a site of rapid turnover. *J Biol Chem* **277**, 15419-15425.
- Anderson MP, Berger HA, Rich DP, Gregory RJ, Smith AE, & Welsh MJ (1991). Nucleoside triphosphates are required to open the CFTR chloride channel. *Cell* **67**, 775-784.
- Basso C, Vergani P, Nairn AC, & Gadsby DC (2003). Prolonged nonhydrolytic interaction of nucleotide with CFTR's NH₂-terminal nucleotide binding domain and its role in channel gating. *J Gen Physiol* **122**, 333-348.
- Bompadre SG, Sohma Y, Li M, & Hwang TC (2007). G551D and G1349D, two CF-associated mutations in the signature sequences of CFTR, exhibit distinct gating defects. *J Gen Physiol* **129**, 285-298.
- Cai Z, Palmai-Pallag T, Khuituan P, Mutolo MJ, Boinot C, Liu B, Scott-Ward TS, Callebaut I, Harris A, & Sheppard DN (2015). Impact of the F508del mutation on ovine CFTR, a Cl⁻ channel with enhanced conductance and ATP-dependent gating. *J Physiol* **593**, 2427-2446.
- Cai Z, Scott-Ward TS, & Sheppard DN (2003). Voltage-dependent gating of the cystic fibrosis transmembrane conductance regulator Cl⁻ channel. *J Gen Physiol* **122**, 605-620.
- Cai Z & Sheppard DN (2002). Phloxedoxin B interacts with the cystic fibrosis transmembrane conductance regulator at multiple sites to modulate channel activity. *J Biol Chem* **277**, 19546-19553.
- Cai Z, Taddei A, & Sheppard DN (2006). Differential sensitivity of the cystic fibrosis (CF)-associated mutants G551D and G1349D to potentiators of the cystic fibrosis transmembrane conductance regulator (CFTR) Cl⁻ channel. *J Biol Chem* **281**, 1970-1977.
- Carson MR, Travis SM, & Welsh MJ (1995). The two nucleotide-binding domains of cystic fibrosis transmembrane conductance regulator (CFTR) have distinct functions in controlling channel activity. *J Biol Chem* **270**, 1711-1717.
- Chen JH, Cai Z, & Sheppard DN (2009). Direct sensing of intracellular pH by the cystic fibrosis transmembrane conductance regulator (CFTR) Cl⁻ channel. *J Biol Chem* **284**, 35495-35506.
- Colquhoun D & Hawkes AG (1982). On the stochastic properties of bursts of single ion channel openings and of clusters of bursts. *Philos Trans R Soc Lond B Biol Sci* **300**, 1-59.
- Cotten JF & Welsh MJ (1999). Cystic fibrosis-associated mutations at arginine 347 alter the pore architecture of CFTR. Evidence for disruption of a salt bridge. *J Biol Chem* **274**, 5429-5435.
- Csanady L, Mihalyi C, Szollosi A, Torocsik B, & Vergani P (2013). Conformational changes in the catalytically inactive nucleotide-binding site of CFTR. *J Gen Physiol* **142**, 61-73.

- 1 Csanady L, Vergani P, & Gadsby DC (2010). Strict coupling between CFTR's catalytic cycle
2 and gating of its Cl⁻ ion pore revealed by distributions of open channel burst durations. *Proc*
3 *Natl Acad Sci USA* **107**, 1241-1246.
- 4 Cui G, Rahman KS, Infield DT, Kuang C, Prince CZ, & McCarty NA (2014). Three charged
5 amino acids in extracellular loop 1 are involved in maintaining the outer pore architecture of
6 CFTR. *J Gen Physiol* **144**, 159-179.
- 7 Dalemans W, Barbry P, Champigny G, Jallat S, Dott K, Dreyer D, Crystal RG, Pavirani A,
8 Lecocq JP, & Lazdunski M (1991). Altered chloride ion channel kinetics associated with the
9 ΔF508 cystic fibrosis mutation. *Nature* **354**, 526-528.
- 10 Dong Q, Ostedgaard LS, Rogers C, Vermeer DW, Zhang Y, & Welsh MJ (2011). Human-
11 mouse cystic fibrosis transmembrane conductance regulator (CFTR) chimeras identify
12 regions that partially rescue CFTR-ΔF508 processing and alter its gating defect. *Proc Natl*
13 *Acad Sci USA* **109**, 8270-8273.
- 14 Fuller MD, Zhang ZR, Cui G, & McCarty NA (2005). The block of CFTR by scorpion
15 venom is state-dependent. *Biophys J* **89**, 3960-3975.
- 16 Gao X & Hwang TC (2015). Localizing a gate in CFTR. *Proc Natl Acad Sci USA* **112**, 2461-
17 2466.
- 18 Haws C, Krouse ME, Xia Y, Gruenert DC, & Wine JJ (1992). CFTR channels in
19 immortalized human airway cells. *Am J Physiol* **263**, L692-L707.
- 20 Hennager DJ, Ikuma M, Hoshi T, & Welsh MJ (2001). A conditional probability analysis of
21 cystic fibrosis transmembrane conductance regulator gating indicates that ATP has multiple
22 effects during the gating cycle. *Proc Natl Acad Sci USA* **98**, 3594-3599.
- 23 Howell LD, Borchardt R, & Cohn JA (2000). ATP hydrolysis by a CFTR domain:
24 pharmacology and effects of G551D mutation. *Biochem Biophys Res Commun* **271**, 518-525.
- 25 Hwang TC & Kirk KL (2013). The CFTR ion channel: gating, regulation, and anion
26 permeation. *Cold Spring Harb Perspect Med* **3**, a009498.
- 27 Hwang TC, Nagel G, Nairn AC, & Gadsby DC (1994). Regulation of the gating of cystic
28 fibrosis transmembrane conductance regulator Cl⁻ channels by phosphorylation and ATP
29 hydrolysis. *Proc Natl Acad Sci USA* **91**, 4698-4702.
- 30 Illek B, Zhang L, Lewis NC, Moss RB, Dong JY, & Fischer H (1999). Defective function of
31 the cystic fibrosis-causing missense mutation G551D is recovered by genistein. *Am J Physiol*
32 **277**, C833-C839.
- 33 Ikuma M & Welsh MJ (2000). Regulation of CFTR Cl⁻ channel gating by ATP binding and
34 hydrolysis. *Proc Natl Acad Sci U S A* **97**, 8675-8680.
- 35 Infield DT, Cui G, Kuang C, & McCarty NA (2016). Positioning of extracellular loop 1
36 affects pore gating of the cystic fibrosis transmembrane conductance regulator. *Am J Physiol*
37 *Lung Cell Mol Physiol* **310**, L403-L414.

- 1 Ishihara H & Welsh MJ (1997). Block by MOPS reveals a conformation change in the CFTR
2 pore produced by ATP hydrolysis. *Am J Physiol* **273**, C1278-C1289.
- 3 Jih KY, Li M, Hwang TC, & Bompadre SG (2011). The most common cystic fibrosis-
4 associated mutation destabilizes the dimeric state of the nucleotide-binding domains of CFTR.
5 *J Physiol* **589**, 2719-2731.
- 6 Jih KY, Sohma Y, Li M, & Hwang TC (2012). Identification of a novel post-hydrolytic state
7 in CFTR gating. *J Gen Physiol* **139**, 359-370.
- 8 Kidd JF, Ramjeesingh M, Stratford F, Huan LJ, & Bear CE (2004). A heteromeric complex
9 of the two nucleotide binding domains of cystic fibrosis transmembrane conductance
10 regulator (CFTR) mediates ATPase activity. *J Biol Chem* **279**, 41664-41669.
- 11 Kienker P (1989). Equivalence of aggregated Markov models of ion-channel gating. *Proc R*
12 *Soc Lond B Biol Sci* **236**, 269-309.
- 13 Lansdell KA, Delaney SJ, Lunn DP, Thomson SA, Sheppard DN, & Wainwright BJ (1998).
14 Comparison of the gating behaviour of human and murine cystic fibrosis transmembrane
15 conductance regulator Cl⁻ channels expressed in mammalian cells. *J Physiol* **508 (Pt 2)**, 379-
16 392.
- 17 Lewis HA, Buchanan SG, Burley SK, Connors K, Dickey M, Dorwart M, Fowler R, Gao X,
18 Guggino WB, Hendrickson WA, Hunt JF, Kearins MC, Lorimer D, Maloney PC, Post KW,
19 Rajashankar KR, Rutter ME, Sauder JM, Shriver S, Thibodeau PH, Thomas PJ, Zhang M,
20 Zhao X, & Emtage S (2004). Structure of nucleotide-binding domain 1 of the cystic fibrosis
21 transmembrane conductance regulator. *EMBO J* **23**, 282-293.
- 22 Li C, Ramjeesingh M, Wang W, Garami E, Hewryk M, Lee D, Rommens JM, Galley K, &
23 Bear CE (1996). ATPase activity of the cystic fibrosis transmembrane conductance regulator.
24 *J Biol Chem* **271**, 28463-28468.
- 25 Mense M, Vergani P, White DM, Altberg G, Nairn AC, & Gadsby DC (2006). In vivo
26 phosphorylation of CFTR promotes formation of a nucleotide-binding domain heterodimer.
27 *EMBO J* **25**, 4728-4739.
- 28 Mornon JP, Lehn P, & Callebaut I (2008). Atomic model of human cystic fibrosis
29 transmembrane conductance regulator: membrane-spanning domains and coupling interfaces.
30 *Cell Mol Life Sci* **65**, 2594-2612.
- 31 Qin F, Auerbach A, & Sachs F (1997). Maximum likelihood estimation of aggregated
32 Markov processes. *Proc Biol Sci* **264**, 375-383.
- 33 Rich DP, Anderson MP, Gregory RJ, Cheng SH, Paul S, Jefferson DM, McCann JD, Klinger
34 KW, Smith AE, & Welsh MJ (1990). Expression of cystic fibrosis transmembrane
35 conductance regulator corrects defective chloride channel regulation in cystic fibrosis airway
36 epithelial cells. *Nature* **347**, 358-363.
- 37 Rich DP, Gregory RJ, Anderson MP, Manavalan P, Smith AE, & Welsh MJ (1991). Effect of
38 deleting the R domain on CFTR-generated chloride channels. *Science* **253**, 205-207.

- 1 Riordan JR, Rommens JM, Kerem B, Alon N, Rozmahel R, Grzelczak Z, Zielenski J, Lok S,
2 Plavsic N, Chou JL, Drumm ML, Iannuzzi MC, Collins FS, & Tsui LC (1989). Identification
3 of the cystic fibrosis gene: cloning and characterization of complementary DNA. *Science* **245**,
4 1066-1073.
- 5 Sakmann B & Trube G (1984). Voltage-dependent inactivation of inward-rectifying single-
6 channel currents in the guinea-pig heart cell membrane. *J Physiol* **347**, 659-683.
- 7 Scott-Ward TS, Cai Z, Dawson ES, Doherty A, Da Paula AC, Davidson H, Porteous DJ,
8 Wainwright BJ, Amaral MD, Sheppard DN, & Boyd AC (2007). Chimeric constructs endow
9 the human CFTR Cl⁻ channel with the gating behavior of murine CFTR. *Proc Natl Acad Sci*
10 *USA* **104**, 16365-16370.
- 11 Scott-Ward TS, Li H, Schmidt A, Cai Z, & Sheppard DN (2004). Direct block of the cystic
12 fibrosis transmembrane conductance regulator Cl⁻ channel by niflumic acid. *Mol Membr Biol*
13 **21**, 27-38.
- 14 Serohijos AW, Hegedus T, Aleksandrov AA, He L, Cui L, Dokholyan NV, & Riordan JR
15 (2008). Phenylalanine-508 mediates a cytoplasmic-membrane domain contact in the CFTR
16 3D structure crucial to assembly and channel function. *Proc Natl Acad Sci USA* **105**, 3256-
17 3261.
- 18 Sheppard DN, Rich DP, Ostedgaard LS, Gregory RJ, Smith AE, & Welsh MJ (1993).
19 Mutations in CFTR associated with mild-disease-form Cl⁻ channels with altered pore
20 properties. *Nature* **362**, 160-164.
- 21 Sheppard DN & Robinson KA (1997). Mechanism of glibenclamide inhibition of cystic
22 fibrosis transmembrane conductance regulator Cl⁻ channels expressed in a murine cell line. *J*
23 *Physiol* **503** (Pt 2), 333-346.
- 24 Sorum B, Czégé D, & Csanády L (2015). Timing of CFTR pore opening and structure of its
25 transition state. *Cell* **163**, 724-733.
- 26 Sunderman ER & Zagotta WN (1999). Mechanism of allosteric modulation of rod cyclic
27 nucleotide-gated channels. *J Gen Physiol* **113**, 601-620.
- 28 Tabcharani JA, Linsdell P, & Hanrahan JW (1997). Halide permeation in wild-type and
29 mutant cystic fibrosis transmembrane conductance regulator chloride channels. *J Gen Physiol*
30 **110**, 341-354.
- 31 Tsai MF, Li M, & Hwang TC (2010). Stable ATP binding mediated by a partial NBD dimer
32 of the CFTR chloride channel. *J Gen Physiol* **135**, 399-414.
- 33 Tsai MF, Shimizu H, Sohma Y, Li M, & Hwang TC (2009). State-dependent modulation of
34 CFTR gating by pyrophosphate. *J Gen Physiol* **133**, 405-419.
- 35 Venglarik CJ, Schultz BD, Frizzell RA, & Bridges RJ (1994). ATP alters current fluctuations
36 of cystic fibrosis transmembrane conductance regulator: evidence for a three-state activation
37 mechanism. *J Gen Physiol* **104**, 123-146.
- 38 Vergani P, Lockless SW, Nairn AC, & Gadsby DC (2005). CFTR channel opening by ATP-
39 driven tight dimerization of its nucleotide-binding domains. *Nature* **433**, 876-880.

- 1 Vergani P, Nairn AC, & Gadsby DC (2003). On the mechanism of MgATP-dependent gating
2 of CFTR Cl⁻ channels. *J Gen Physiol* **121**, 17-36.
- 3 Winter MC, Sheppard DN, Carson MR, & Welsh MJ (1994). Effect of ATP concentration on
4 CFTR Cl⁻ channels: a kinetic analysis of channel regulation. *Biophys J* **66**, 1398-1403.
- 5 Winter MC & Welsh MJ (1997). Stimulation of CFTR activity by its phosphorylated R
6 domain. *Nature* **389**, 294-296.
- 7 Zegarra-Moran O, Monteverde M, Galiotta LJ, & Moran O (2007). Functional analysis of
8 mutations in the putative binding site for cystic fibrosis transmembrane conductance
9 regulator potentiators. Interaction between activation and inhibition. *J Biol Chem* **282**, 9098-
10 9104.
- 11 Zeltwanger S, Wang F, Wang GT, Gillis KD, & Hwang TC (1999). Gating of cystic fibrosis
12 transmembrane conductance regulator chloride channels by adenosine triphosphate
13 hydrolysis. Quantitative analysis of a cyclic gating scheme. *J Gen Physiol* **113**, 541-554.
- 14 Zhou Z, Hu S, & Hwang TC (2001). Voltage-dependent flickery block of an open cystic
15 fibrosis transmembrane conductance regulator (CFTR) channel pore. *J Physiol* **532**, 435-448.

COMPETING INTERESTS

None.

AUTHOR CONTRIBUTIONS

JH Chen conceived and designed experiments, acquired, analysed and interpreted most data and wrote the article. W Xu acquired and analysed some data. DN Sheppard planned the experiments, contributed to data interpretation and revised the manuscript. DN Sheppard, W Xu and JH Chen all concur with the final submitted version of the manuscript and confirm that all persons designated as authors qualify for authorship, and all those who qualify for authorship are listed. Most data were acquired and analysed at the University of Bristol; some data were acquired and analysed at the University of Hong Kong.

FUNDING

This work was supported by grants from the Cystic Fibrosis Trust grants to DNS and Hong Kong Research Grant Council (ECS#HKU 789713M and GRF#17106315) and National Natural Science Foundation of China (NSFC#31370765 and #81570001) to JHC. During part of this study, JHC was supported by the University of Bristol and an Overseas Research Student award from Universities UK. WX was a recipient of the Lee Shau Kee Postgraduate Fellowship at University of Hong Kong.

ACKNOWLEDGEMENTS

We thank LJV Galletta, CR O’Riordan and MJ Welsh for generous gifts of reagents and WH Franklin (Frequency Devices Inc.), JC Chen and our departmental colleagues for valuable discussions.

1 **Table 1.** Burst analysis of wild-type CFTR gating at different pHi.

Experiment	P _o	MBD	IBI	N
pHi 5.8	0.37 ± 0.01*	361 ± 39*	534 ± 41*	6
pHi 6.3	0.66 ± 0.02*	358 ± 37*	107 ± 10*	6
pHi 7.3 (control)	0.44 ± 0.01	134 ± 4	154 ± 4	15
pHi 8.3	0.31 ± 0.03*	85 ± 7*	205 ± 18*	8
pHi 8.8	0.40 ± 0.01*	93 ± 6*	144 ± 10*	6

- 2 Kinetic parameters: P_o, open probability; MBD, mean burst duration; IBI, interburst interval.
- 3 Data are means ± S.E.M.; *, $P < 0.05$ vs. pHi 7.3 (control), one-way ANOVA. The Table
- 4 includes data that were previously reported (Chen *et al.*, 2009).

1 **Table 2.** Comparison of kinetic parameters derived using pCLAMP and QuB software.

pH _i 6.3								
(N = 6)	P _o		P _{o-burst}		MBD (ms)		IBI (ms)	
Model / pH _i	7.3	6.3	7.3	6.3	7.3	6.3	7.3	6.3
pCLAMP	0.47±0.02	0.66±0.02*	0.95±0.01	0.87±0.02*	147±5	358±37*	153±9	107±10*
C ₁ ↔O↔C ₂	0.47±0.02	0.68±0.02*	0.93±0.01	0.85±0.02*	132±4	315±30*	135±7	84±8*
C ₁ ↔C ₂ ↔O	0.47±0.02	0.69±0.02*	0.93±0.01	0.87±0.01*	137±5	326±21*	137±9	83±7*
pH _i 5.8								
(N = 6)	P _o		P _{o-burst}		MBD (ms)		IBI (ms)	
Model / pH _i	7.3	5.8	7.3	5.8	7.3	5.8	7.3	5.8
pCLAMP	0.41±0.02	0.37±0.01*	0.95±0.01	0.92±0.02*	127±6	361±39*	169±11	534±41*
C ₁ ↔O↔C ₂	0.43±0.01	0.37±0.02*	0.92±0.01	0.89±0.02*	113±3	299±19*	138±10	433±45*
C ₁ ↔C ₂ ↔O	0.42±0.01	0.38±0.02*	0.92±0.01	0.89±0.01*	117±3	297±17*	143±9	412±44*

2 P_{o-burst}, P_o within a burst. Data are means ± S.E.M. of N observations; *, *P* < 0.05 vs. pH_i 7.3
3 (control), paired Student's *t*-test. Data from pCLAMP software were obtained by burst
4 analysis and time constant measurements using the event lists from CFTR single-channel
5 recordings (see Methods for details). Data from QuB software were derived using the rate
6 constants in the C₁ ↔ C₂ ↔ O and C₁ ↔ O ↔ C₂ kinetic schemes (Fig. 4) with Equations 2
7 and 3 (see text for details). Only membrane patches that contained a single CFTR Cl⁻
8 channel were used for analysis. See Table 1 for other details.

1 **Table 3.** Comparison of time constants derived using pCLAMP and QuB software.

pH _i 6.3						
(N = 6)	τ_o (ms)		τ_{cf} (ms)		τ_{cs} (ms)	
Model / pH _i	7.3	6.3	7.3	6.3	7.3	6.3
pCLAMP	48±3	38±5*	3.1±0.2	4.9±0.4*	136±11	84±8*
C ₁ ↔O↔C ₂	42±3	31±4*	3.2±0.2	4.7±0.5*	135±70	84±8*
C ₁ ↔C ₂ ↔O	39±5	33±4	3.2±0.2	4.6±0.5*	137±90	83±7*
pH _i 5.8						
(N = 6)	τ_o (ms)		τ_{cf} (ms)		τ_{cs} (ms)	
Model / pH _i	7.3	5.8	7.3	5.8	7.3	5.8
pCLAMP	46±5	50±7	3.2±0.2	4.4±0.2*	154±14	487±51*
C ₁ ↔O↔C ₂	38±4	39±5	3.2±0.1	4.4±0.2*	138±10	433±45*
C ₁ ↔C ₂ ↔O	38±4	39±5	3.3±0.1	4.5±0.3*	143±90	412±44*

2 Data are means ± S.E.M. of N observations; *, $P < 0.05$ vs. pH_i 7.3 (control), paired Student's t-

3 test. See Figure 2 and Table 2 for other details.

FIGURES AND LEGENDS

Figure 1. Altering pH_i affects the intraburst activity of wild-type CFTR. **A and B**, representative recordings show the single-channel activity of a wild-type CFTR channel at pH_i 8.3, 7.3 and 6.3 (A) or at pH_i 8.8, 7.3 and 5.8 (B) in the presence of ATP (0.3 mM) and PKA (75 nM). Dotted lines indicate where the channel was closed and downward deflections correspond to channel openings. The recordings in (A) and (B) are from separate wild-type CFTR Cl^- channels in different excised inside-out membrane patches.

Figure 2. Multiple effects of pH_i on wild-type CFTR channel gating. **A-B**, open- (A) and closed-time (B) histograms of a wild-type CFTR channel at pH_i 6.3, 7.3 and 8.3. Vertical lines show the open-time constant τ_o , fast closed-time constant τ_{cf} , and slow closed-time constant τ_{cs} . The continuous coloured lines are the fits of one- or two-component exponential functions to the data. The dotted black lines in the closed-time histograms show the individual components of the functions. Logarithmic x-axes with 10 bins per decade were used for the dwell-time histograms. **C-D**, open- (C) and closed-time (D) histograms from a different wild-type CFTR channel tested at pH_i 5.8, 7.3 and 8.8; other details as for (A) and (B). **E-G**, effects of acidic (yellow) and alkaline (green) pH_i on τ_o , τ_{cf} and τ_{cs} . Data are means \pm S.E.M. Numbers in parentheses indicate N for panels E-G; *, $P < 0.05$ vs. pH_i 7.3 (control), one-way ANOVA. Error bars are smaller than symbol size except where shown.

Figure 3. Biological buffers are without effect on CFTR intraburst gating. **A-C**, effects on MBD, τ_o and τ_{cf} of pH_i solutions containing 3-fold concentration increases in Trizma or Bis-Tris buffers. Circles joined by lines show values from individual experiments and columns are means \pm S.E.M. Data are from membrane patches that contained one or two active CFTR Cl^- channels. **D-G**, effects on MBD, τ_o , τ_{cf} and τ_{cs} of different buffer solutions. Circles show

values from individual experiments and columns are means + S.E.M. For Trizma/Bis-Tris and TES groups, membrane patches that contained only one active CFTR Cl^- channel were used for analysis. Numbers in parentheses indicate N for panels A-C and D-G. Statistical differences between groups were analyzed by paired Student's t-test (A-C) and one-way ANOVA (D-G).

Figure 4. Kinetic modeling of CFTR gating using linear three-state schemes. **A and F**, the $\text{C}_1 \leftrightarrow \text{O} \leftrightarrow \text{C}_2$ and the $\text{C}_1 \leftrightarrow \text{C}_2 \leftrightarrow \text{O}$ kinetic schemes. States, C_1 , C_2 and O represent two closed states and one open state, respectively, while β_1 , β_2 , α_1 and α_2 represent the rate constants describing transitions between the different states. States enclosed within the dashed box represent the bursting state. **B-E**, rate constants at acidic (yellow) and alkaline (green) pH_i values for the $\text{C}_1 \leftrightarrow \text{O} \leftrightarrow \text{C}_2$ kinetic scheme. **G-J**, rate constants at acidic (yellow) and alkaline (green) pH_i values for the $\text{C}_1 \leftrightarrow \text{C}_2 \leftrightarrow \text{O}$ kinetic scheme. Data are means \pm S.E.M. Numbers in parentheses indicate N for panels B-E and G-J; *, $P < 0.05$ vs. pH_i 7.3 (control), one-way ANOVA. Error bars are smaller than symbol size except where shown.

Figure 5. Effects of pH_i 6.3 on ATP-dependence of CFTR gating. **A**, representative recordings show the effects of pH_i 6.3 on the single-channel activity of wild-type CFTR at 0.03 and 1 mM ATP. Dotted lines indicate the closed state and downward deflections correspond to channel openings. For representative recordings at 0.3 mM ATP, please see Figure 1A. **B-I**, effects of pH_i 6.3 on MBD, the time constants τ_o , τ_{cf} and τ_{cs} and the rate constants β_1 , β_2 , α_1 and α_2 for the $\text{C}_1 \leftrightarrow \text{O} \leftrightarrow \text{C}_2$ kinetic scheme at the indicated ATP concentrations. Data are means \pm S.E.M. Numbers in parentheses indicate N for panels B-I; *, $P < 0.05$ vs. pH_i 7.3 (control), paired Student's t-test; #, $P < 0.05$ between the indicated

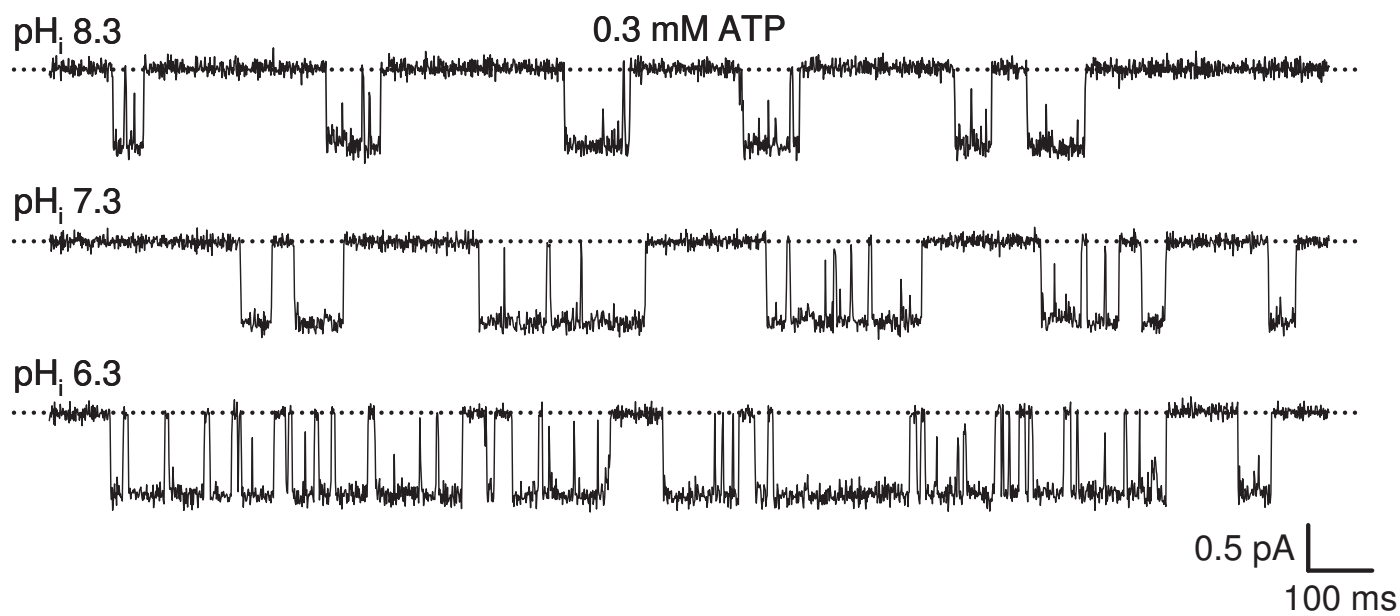
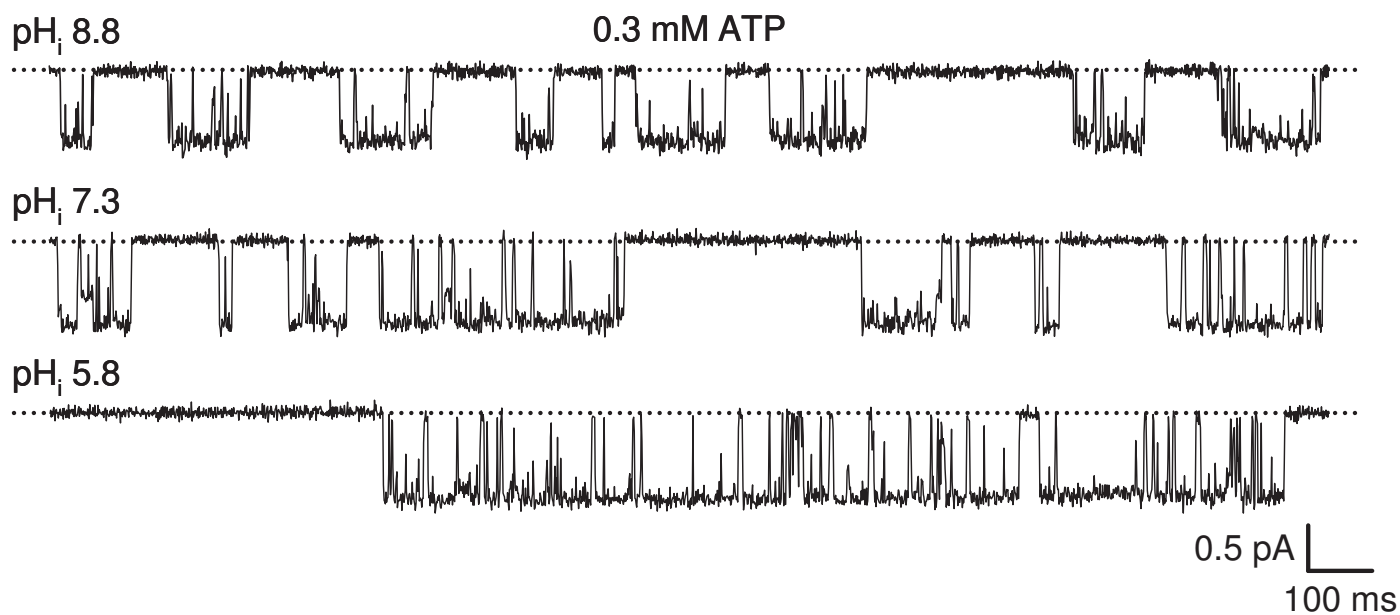
groups of data, one-way ANOVA. Error bars are smaller than symbol size except where shown.

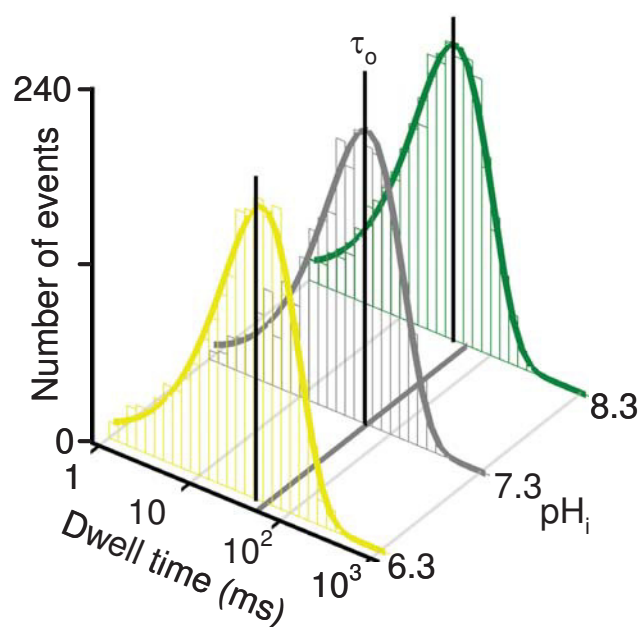
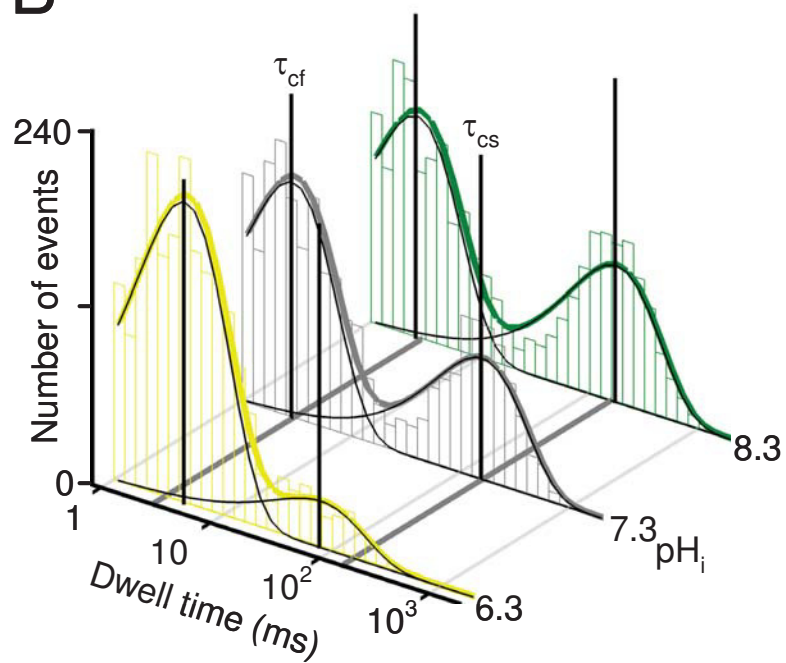
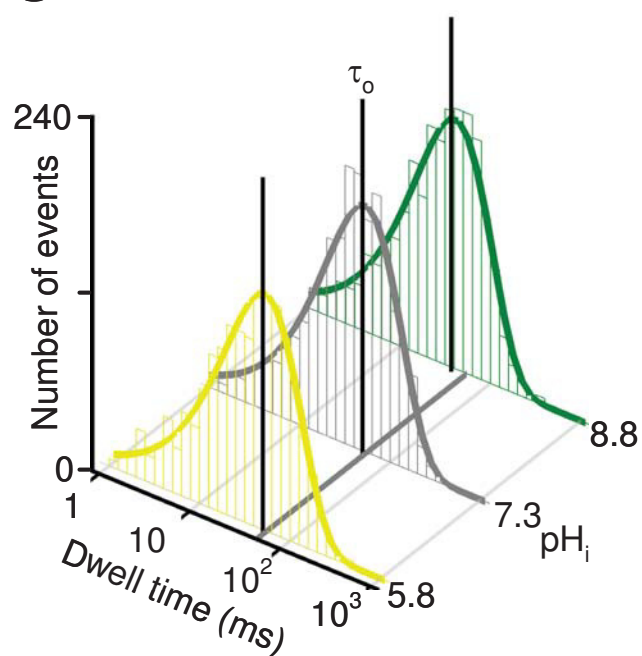
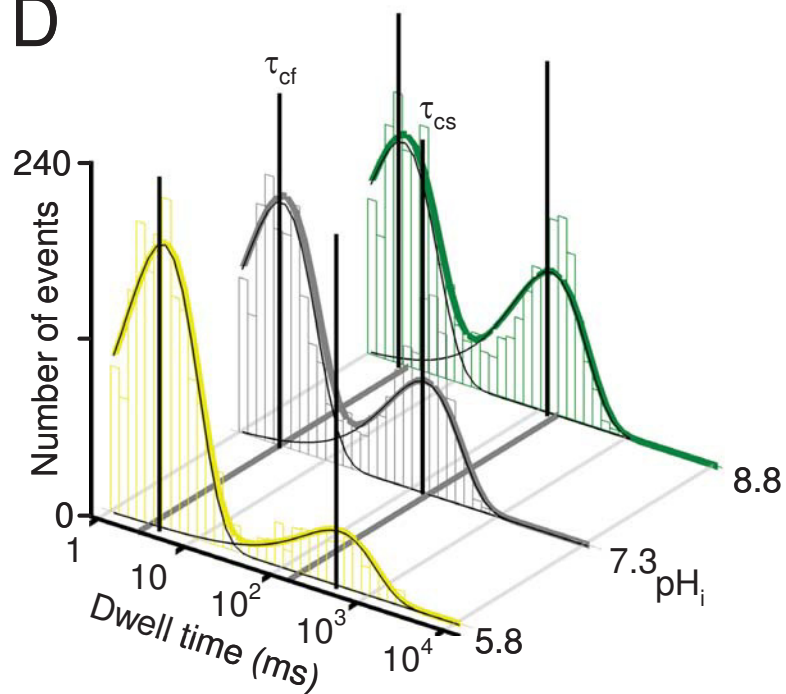
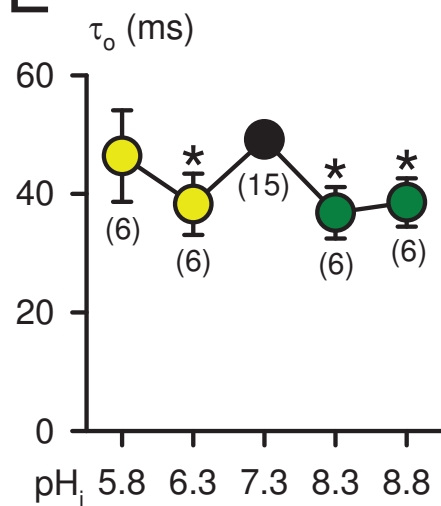
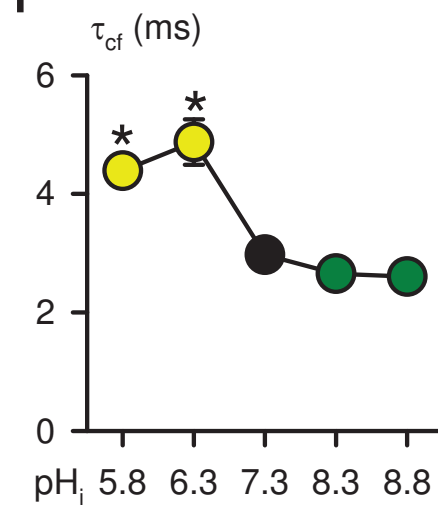
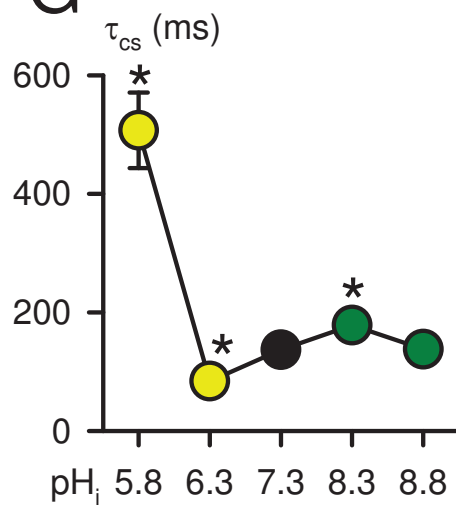
Figure 6. Role of the R domain in CFTR intraburst gating. **A**, representative recordings show the single-channel activity of wild-type and Δ RS660A-CFTR in the presence of 0.3 mM ATP at pH_i 7.3 and pH_i 6.3. **B and C**, the time constants τ_o (B) and τ_{cf} (C) at indicated pH_i values. Data are means + S.E.M. Numbers in parentheses indicate N for panels B and C; *, $P < 0.05$ vs. pH_i 7.3 (control), paired Student's t-test; #, $P < 0.05$ between the indicated groups of data, one-way ANOVA.

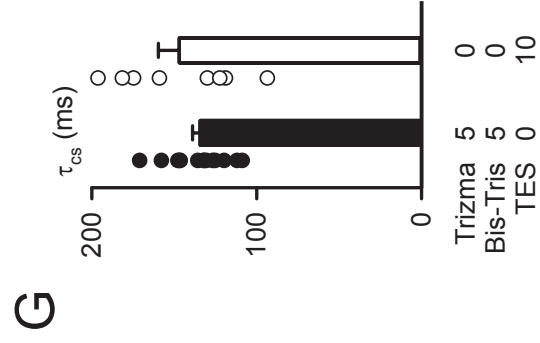
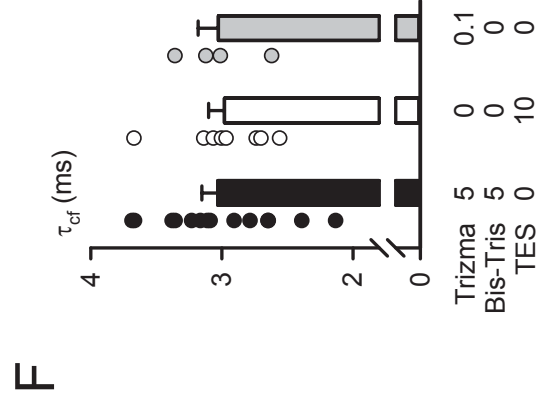
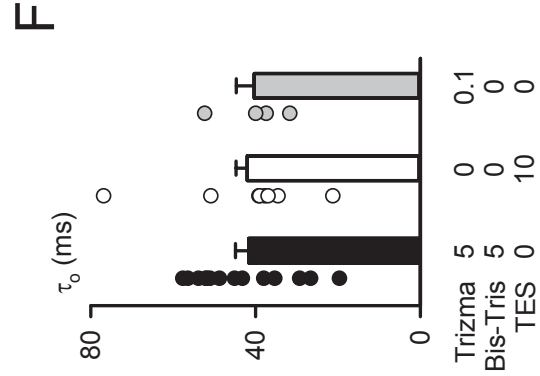
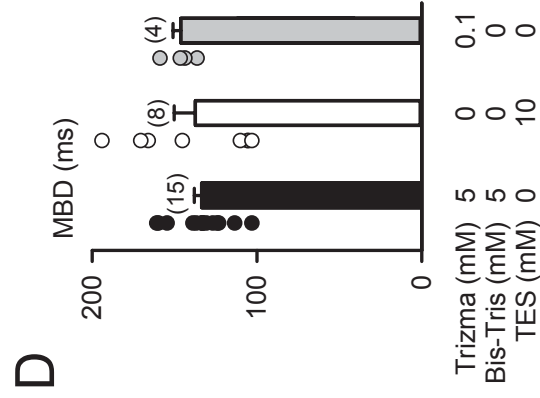
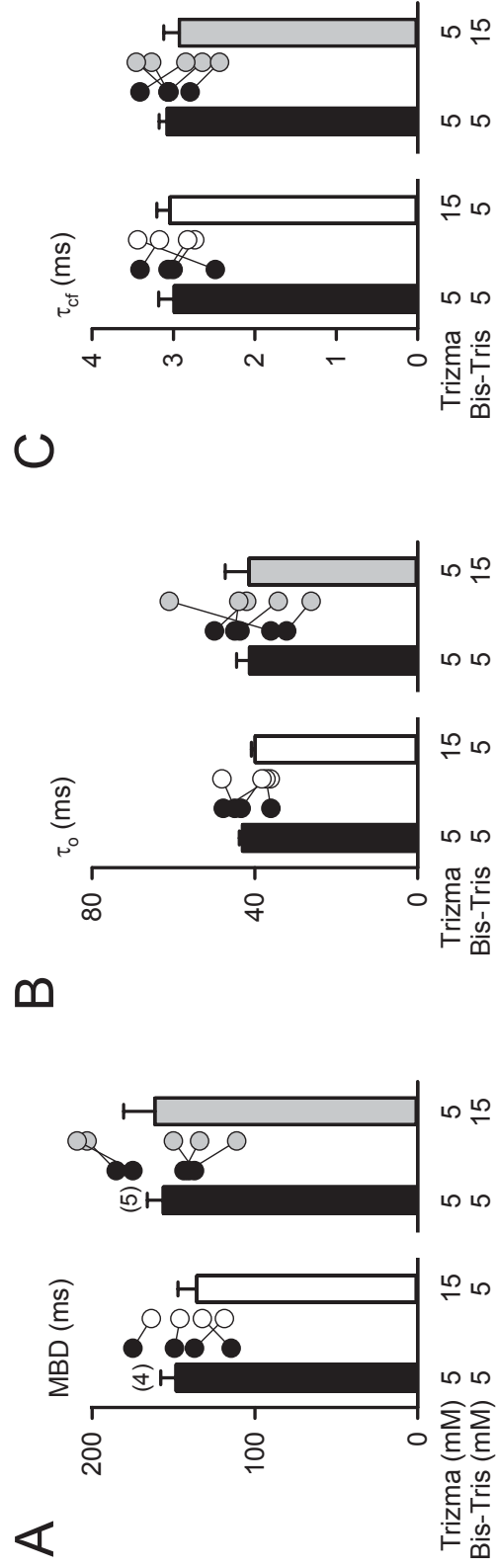
Figure 7. Regulation of CFTR intraburst gating by ATP-binding sites. **A**, representative recordings show the single-channel activity of the indicated CFTR mutants in the presence of 1 mM ATP at pH_i 7.3 and pH_i 6.3. **B and C**, the time constants τ_o (B) and τ_{cf} (C) of different CFTR mutants at the indicated pH_i values. Data are means + S.E.M. Numbers in parentheses indicate N for panels B and C; *, $P < 0.05$ vs. pH_i 7.3 (control), paired Student's t-test; #, $P < 0.05$ between the indicated groups of data, one-way ANOVA.

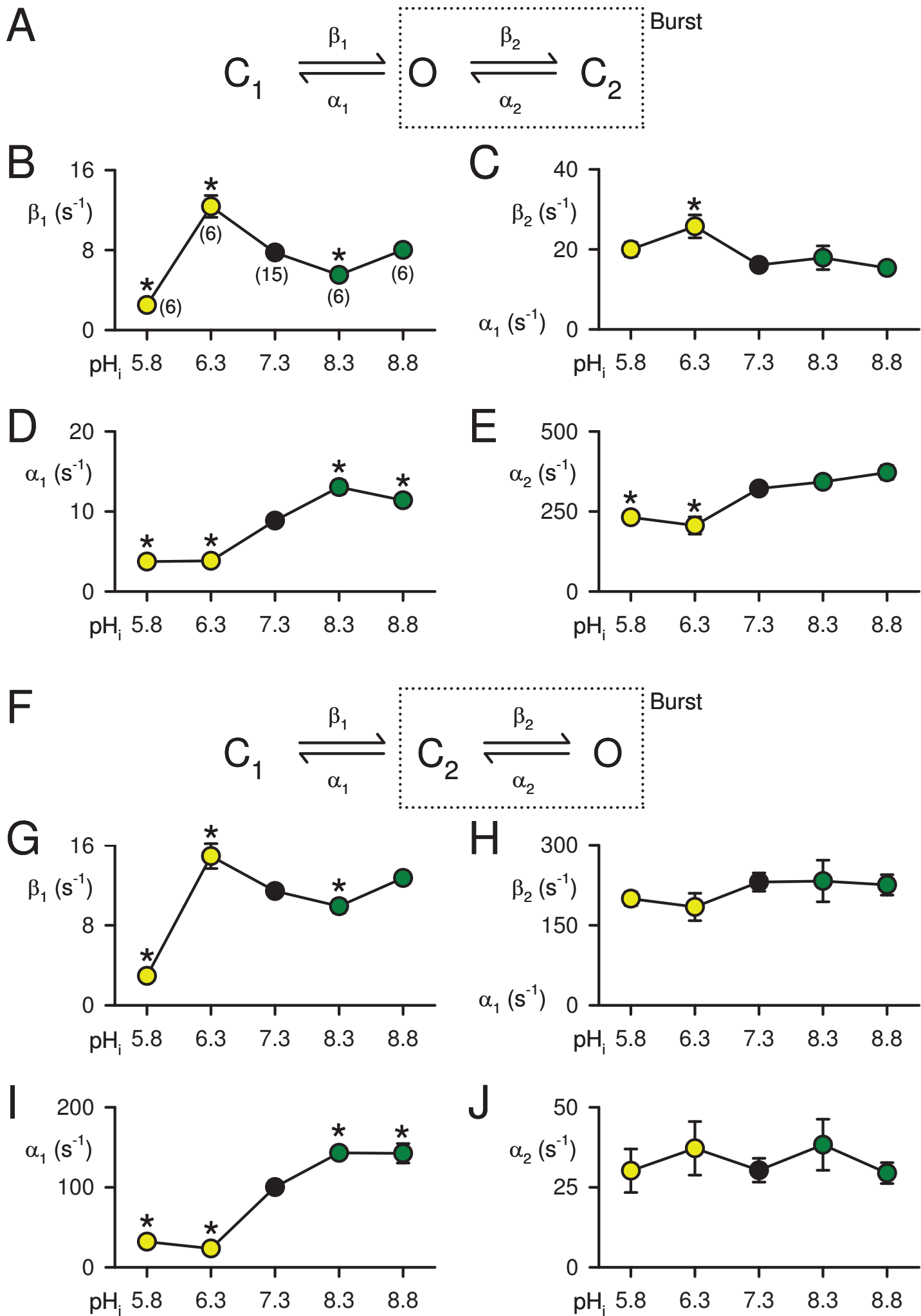
Figure 8. Intraburst gating of the CF mutants G551D-, G1349D- and Δ F508-CFTR. **A**, representative single-channel recordings of the indicated CF mutants in the presence of 1 mM ATP. Left traces show 10-s recordings; right the 1-s portions indicated by grey bars are shown on an expanded time scale. Note that the number of active channels in the G551D- and G1349D-CFTR traces is unknown. For representative control recordings of wild-type CFTR at pH_i 7.3 and 6.3, please see Figure 7A. **B-E**, MBD, τ_o , τ_{cf} and the MBD/ τ_o ratio of CF mutants at pH_i 7.3 and pH_i 6.3. Data are means + S.E.M. Numbers in parentheses

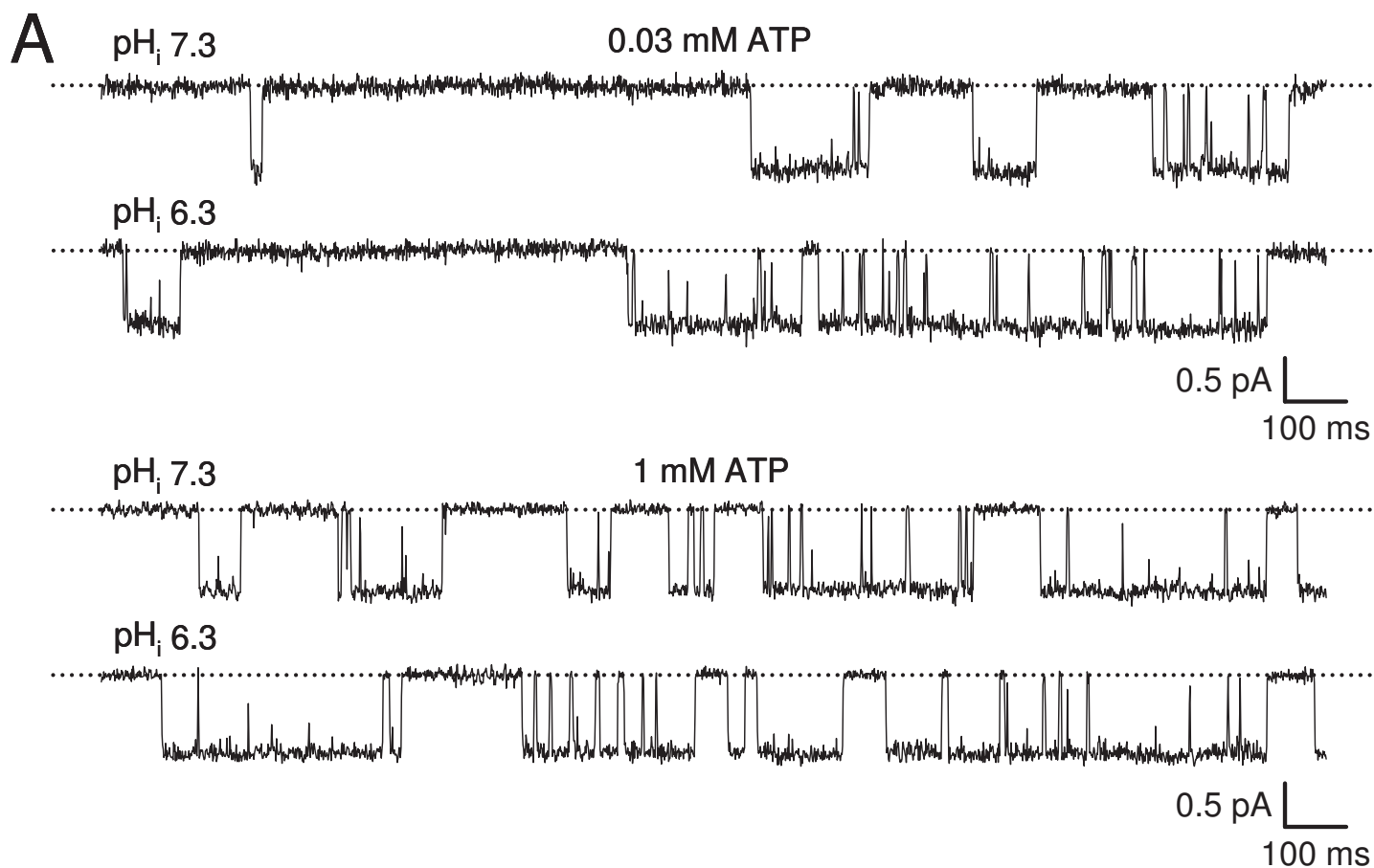
- 1 indicate N for panels B-E; *, $P < 0.05$ vs. pH_i 7.3 (control), paired Student's t-test; #, $P <$
- 2 0.05 between the indicated groups of data, one-way ANOVA.
- 3

A**B**

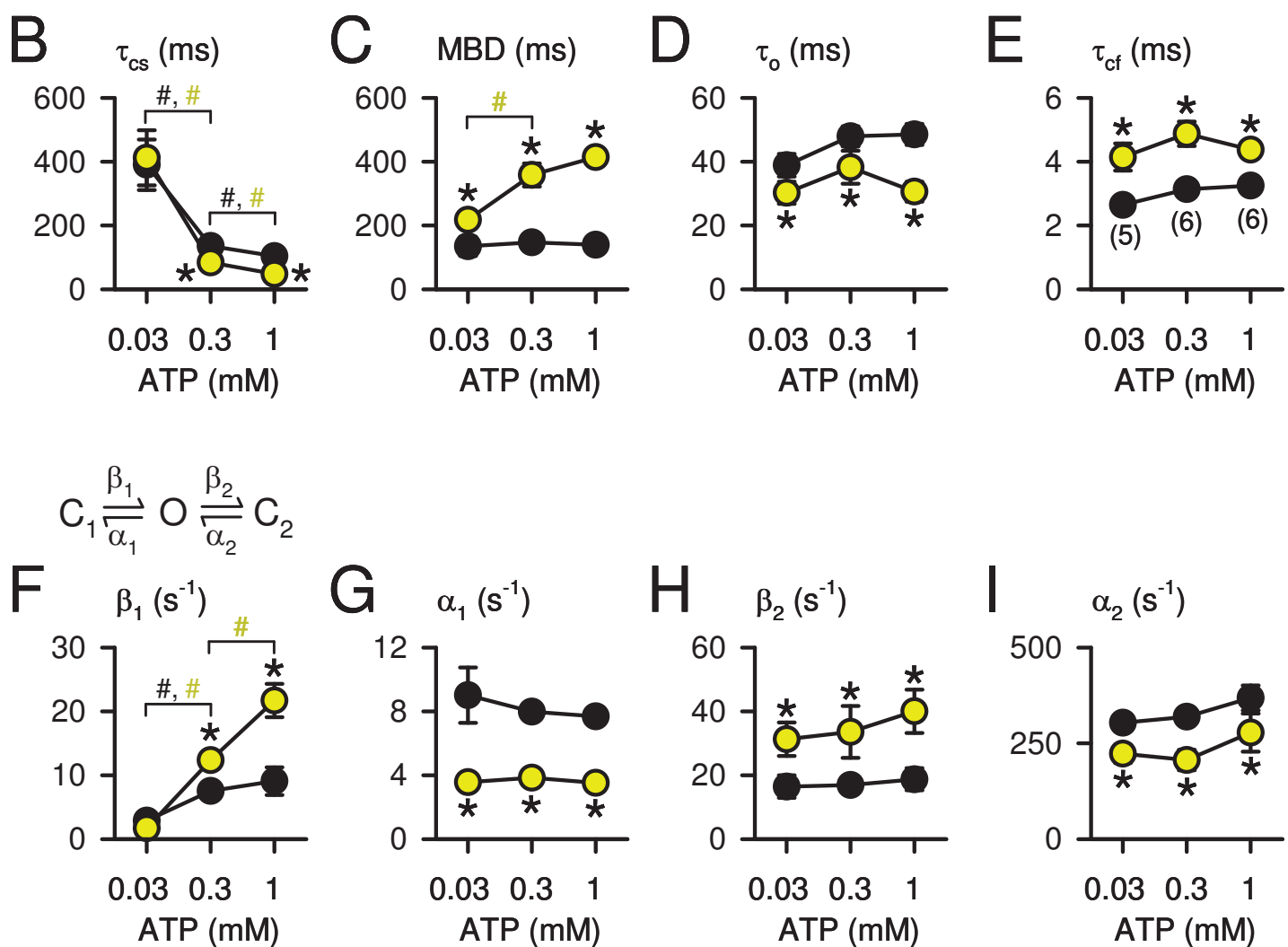
A**B****C****D****E****F****G**

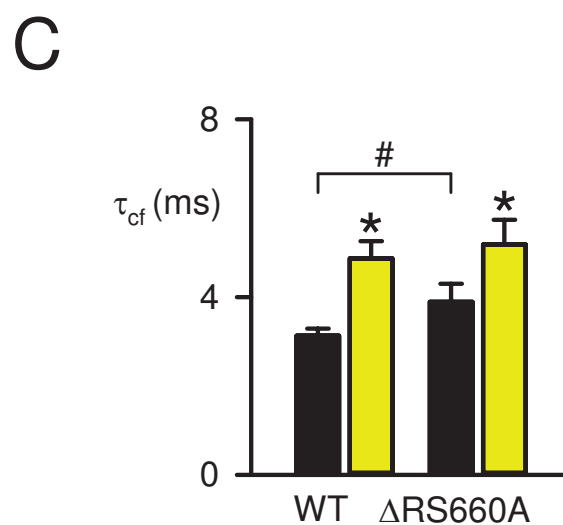
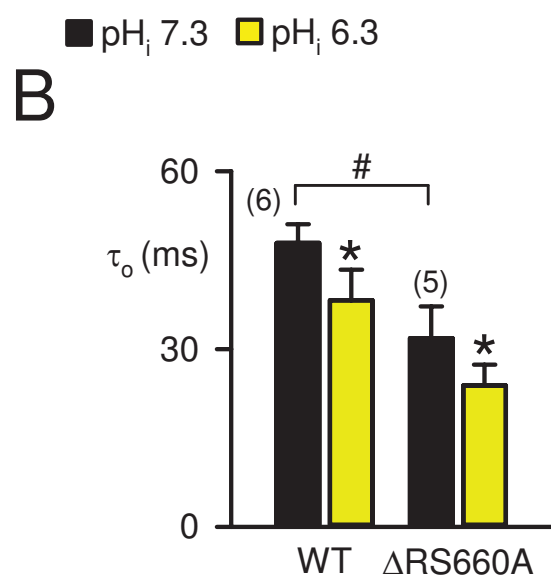
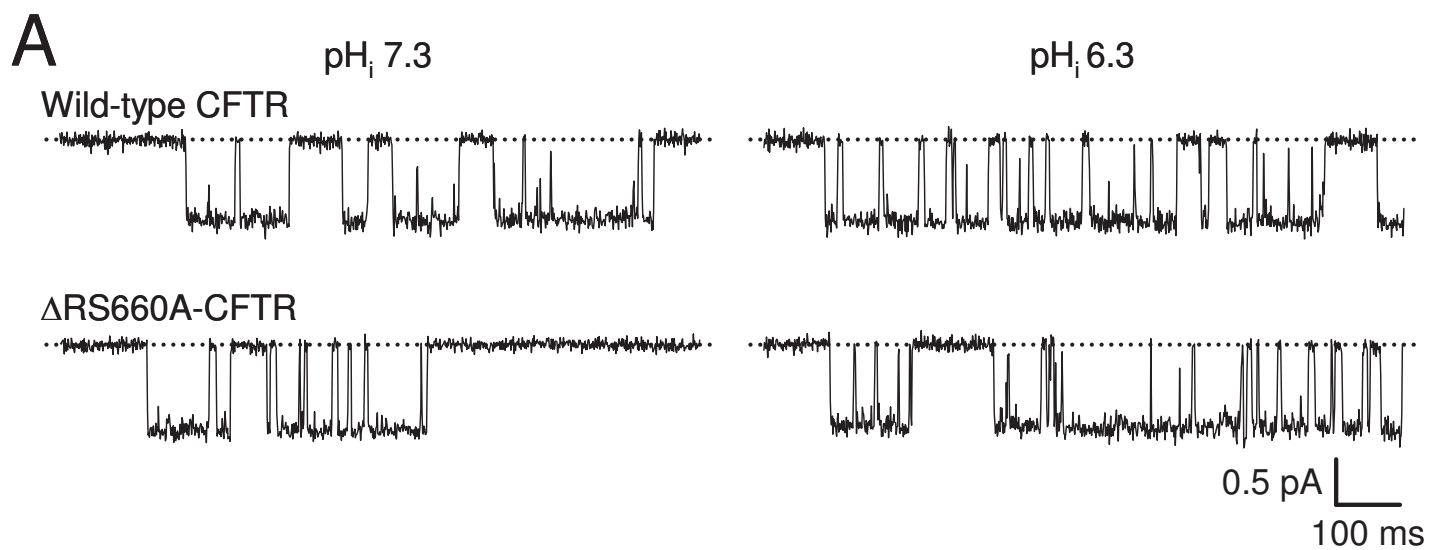


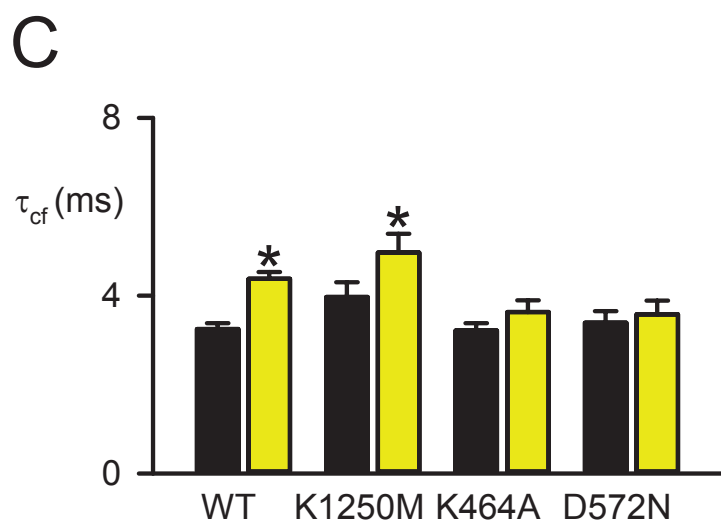
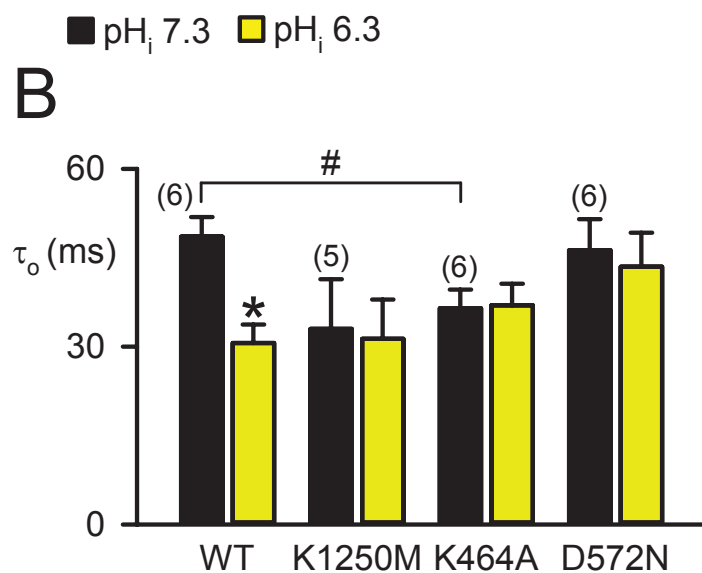
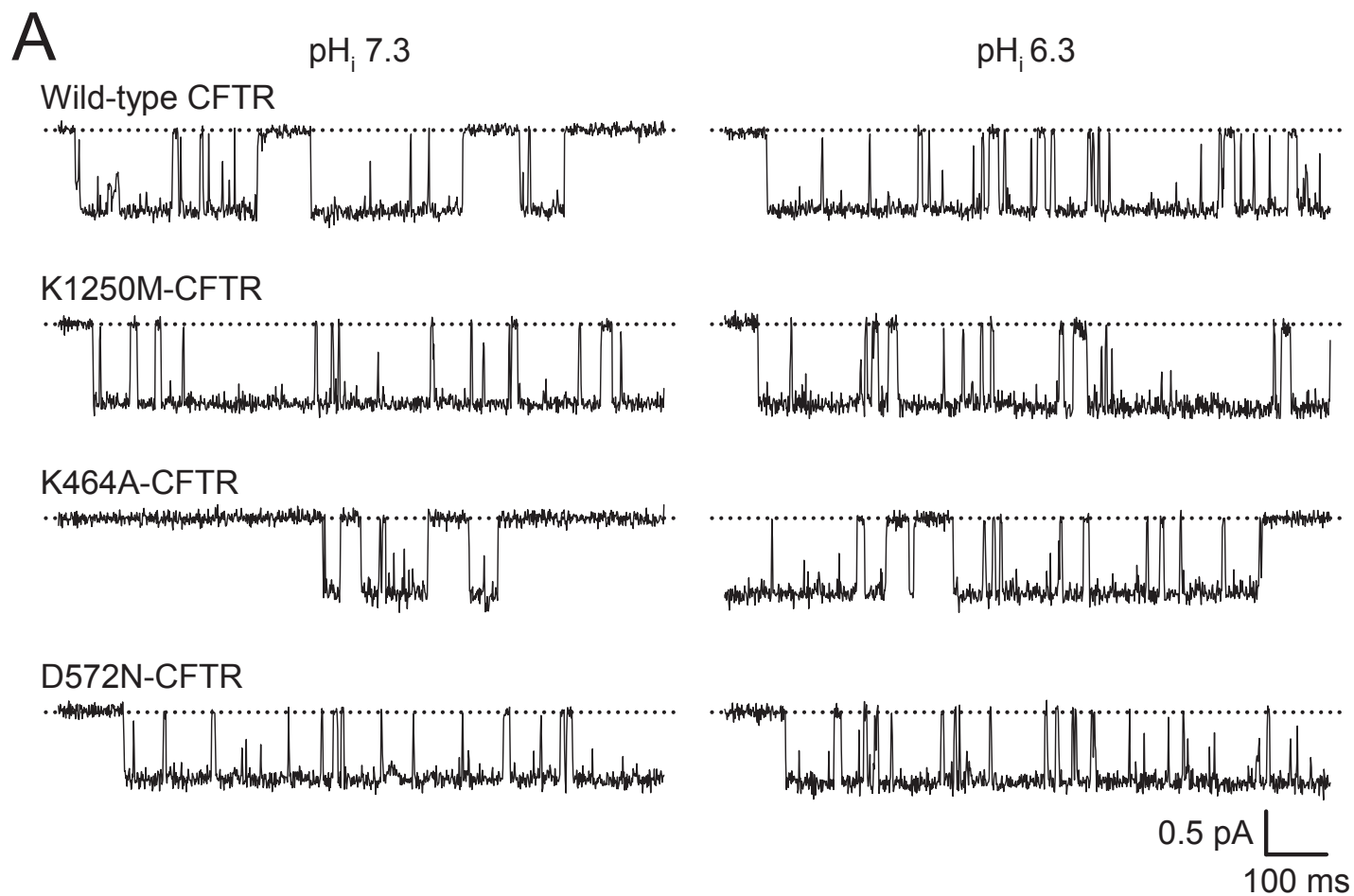


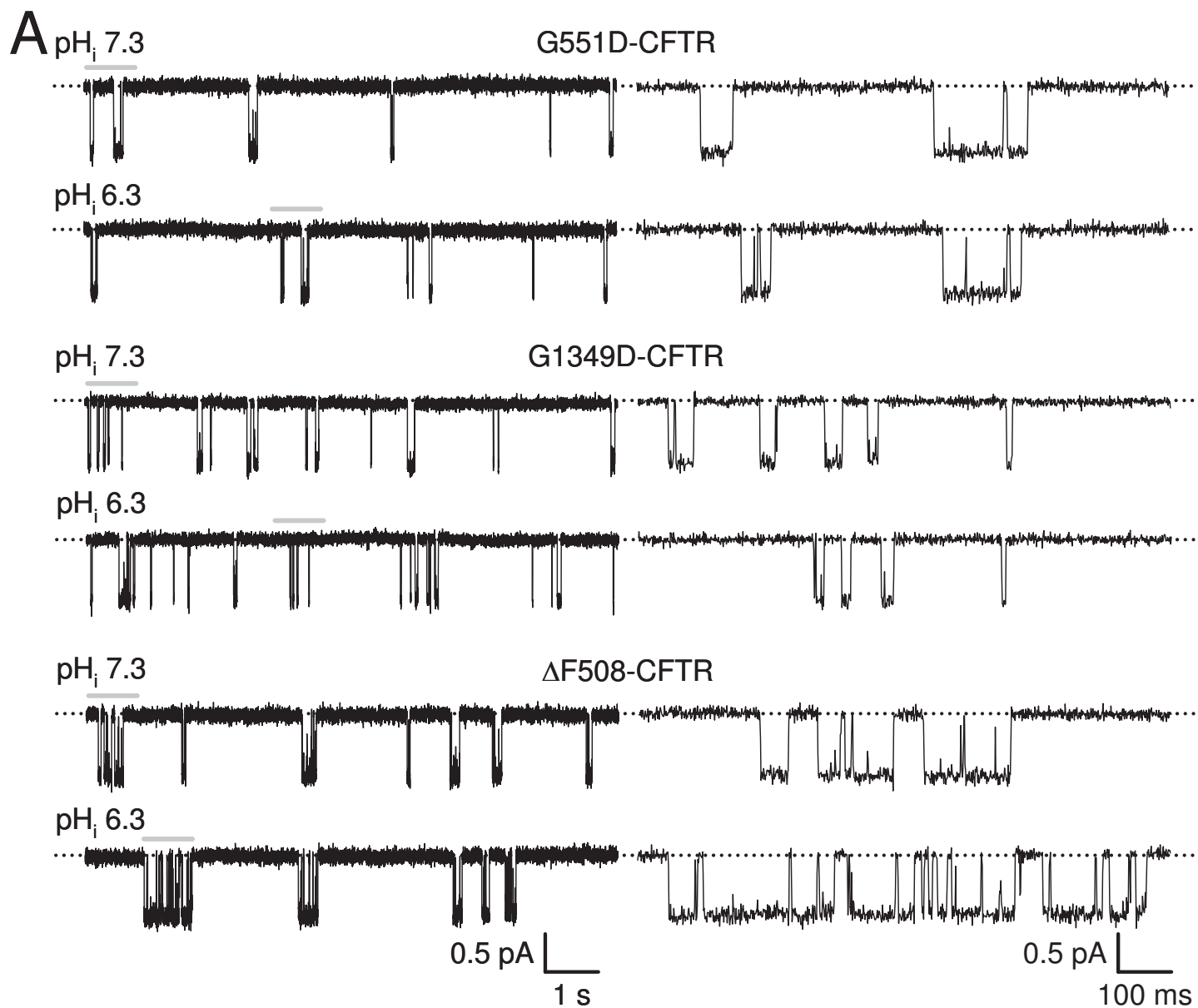


● pH_i 7.3 ● pH_i 6.3









■ pH_i 7.3 ■ pH_i 6.3

